Review of Palaeobotany and Palynology 237 (2017) 37–61

Contents lists available at ScienceDirect

Review of Palaeobotany and Palynology

journal homepage: www.elsevier.com/locate/revpalbo

New petrified calamitaleans from the Permian of the Parnaíba Basin, central-north Brazil, part II, and phytogeographic implications for late Paleozoic floras

Rodrigo Neregato [a,*], Ronny Rößler [b,c], Roberto Iannuzzi [d], Robert Noll [e], Rosemarie Rohn [f]

[a] UNESP – Rio Claro, Post Graduation Program in Regional Geology, Institute of Geosciences and Exact Science, Postal Code: 13506-900 Rio Claro, São Paulo, Brazil
[b] Museum für Naturkunde, Moritzstraße 20, D–09111 Chemnitz, Germany.
[c] TU Bergakademie Freiberg, Geological Institute, Bernhard-von Cotta Straße 2, D–09596 Freiberg, Germany
[d] Department of Paleontology and Stratigraphy, Institute of Geosciences, Universidade Federal do Rio Grande do Sul, Caixa Postal 15.001, Postal Code: 91.509-900, Porto Alegre, Brazil
[e] In den Birkengärten 30, D–67311 Tiefenthal, Germany
[f] UNESP – Rio Claro, Department of Applied Geology, Institute of Geosciences and Exact Science, Caixa Postal 178, Postal Code: 13506-900, Rio Claro, São Paulo, Brazil

ARTICLE INFO

Article history:
Received 15 December 2015
Received in revised form 9 November 2016
Accepted 9 November 2016
Available online 13 November 2016

Keywords:
Sphenophyte anatomy
Growth architecture
Plant interactions
Permian phytogeography

ABSTRACT

Continuing palaeofloristic studies in the Northern Tocantins Fossil Forest, we describe two new calamitalean species from the Permian of the Parnaíba Basin (central-north Brazil). The fossils comprise axes of various sizes, preserved anatomically as siliceous petrifactions, and found in highly mature sandy fluvial deposits of the Motuca Formation. Based on anatomical and morphological characteristics, *Arthropitys tocantinensis* sp. nov. and *Arthropitys barthelii* sp. nov. are described. They share a small central pith cavity (extremely reduced in the latter), scalariform tracheid pitting, and prominent pitting of the ray parenchyma. However, they differ markedly in their branching system: the former having 3–12 branches per node either with or lacking secondary growth, the latter showing 2–17 branches without any secondary growth. However, in *A. tocantinensis* sp. nov., the presence of large woody branches supports a more complex architecture with at least three successive orders of branches. The extensive secondary tissue in both species is homogeneous; clear segmentation is only visible in the proximal wood of *A. tocantinensis* sp. nov., but completely absent in *A. barthelii* sp. nov.

The growth architecture of these upright growing, self-supporting trunks are reconstructed based on sizable transverse and longitudinal preparations. Our results confirm that thick woody calamitaleans were elements of disturbed riparian vegetation and much more diverse in terms of anatomy and branching patterns than previously thought. They were well adapted to seasonally dry conditions and formed major plant constituents of Permian low-latitude Southern Hemisphere communities. Additionally, we report the first evidence of colonisation on arborescent calamitaleans by herbaceous sphenophyte axes from the Permian. One of the *Arthropitys* stems hosts at least 30 *Sphenophyllum* shoots of various ontogenetic stages, growing inside the destroyed pith, which was previously excavated by arthropod boring.

Based on the distribution of key genera within late Paleozoic floras of Euramerica, Gondwana and Cathaysia floral realms cluster analysis and Jaccard Coefficient highlight the distribution of a "Mid-North Brazilian" phytogeographic Region during the early Permian.

1. Introduction

Petrified plants from the Permian of Brazil have been mentioned in the literature for almost one and a half centuries (Brongniart, 1872). However, only the most common psaroniaceous tree ferns, such as the nearly cosmopolitan *Psaronius* or the Southern Hemisphere *Tietea* have been studied in detail (Solms-Laubach, 1913; Herbst, 1985, 1992, 1999). Despite the long history of paleobotanical research in Brazil, the first record of three-dimensionally preserved calamitaleans appeared only 30 years ago. Coimbra and Mussa (1984) identified *Arthropitys*, the most common petrified sphenophyte genus, among several new finds from the Parnaíba Basin of north-central Brazil and erected *Arthropitys cacundensis* Mussa and Coimbra, 1984. Although the small stem or branch fragment found in the Cacunda River, situated between Araguaína (TO) and Carolina (MA), left no doubt regarding the identification at generic level, its size and preservation were hardly adequate to be discussed at specific level, especially in comparison to more

* Corresponding author.
E-mail addresses: rodrigoneregato@hotmail.com (R. Neregato), roessler@naturkunde-chemnitz.de (R. Rößler), roberto.iannuzzi@ufrgs.br (R. Iannuzzi), r.h.noll@t-online.de (R. Noll), rohn@rc.unesp.br (R. Rohn).

http://dx.doi.org/10.1016/j.revpalbo.2016.11.001
0034-6667/

comprehensively characterised species, such as *Arthropitys communis* (Binney) Renault, 1896, *A. deltoides* Cichan and Taylor, 1983 or more recently the type species of the genus, *Arthropitys bistriata* (Cotta) Goeppert *emend*. Rößler et al., 2012.

During the last decade, exposures of the extensive fluvial depositional complex of the Motuca Formation revealed not only new aspects of late Paleozoic vegetational diversity and distribution, but also insights into intra-Permian environmental and climatic development. The border region of southern Maranhão State and northern Tocantins State has yielded numerous large and well-preserved plant fossils, which have expanded our knowledge of low-latitude Gondwanan palaeofloras (Rößler and Noll, 2002; Rößler and Galtier, 2002a,b, 2003; Rößler, 2006). Recently, several detailed studies have shed light on taphonomic or palaeoenvironmental aspects of the host strata (Capretz and Rohn, 2013; Tavares et al., 2014) and initiated systematic investigations of additional plant groups, such as gymnosperms (Kurzawe et al., 2013a,b). Still under open nomenclature, Rößler and Noll (2002) and Neregato (2012) described several new calamitalean forms based on numerous specimens that reveal not only information on anatomy and branching characteristics of their aerial parts, but also initial rooting structures. During field work in 2006, two large woody calamite trunks were excavated revealing clear evidence of basal stems with attached roots. Providing new information on calamitalean root systems in general, Rößler (2014) and Rößler et al. (2014) compared them with similar in-situ rooting forms from the Chemnitz Fossil Lagerstätte in eastern Germany and characterised some of the common Permian species as free-stemmed woody trees anchored in the former soil substrate by numerous secondary roots arising from multiple nodes of the enlarged trunk base and branching several times on their oblique downward course. Neregato et al. (2015) initiated systematic description of new calamitalean species from the Panaíba Basin and introduced *Arthropitys isoramis* and *Arthropitys iannuzzii*.

That fieldwork and the newly discovered fossil sites in the northern part of Tocantins State emphasized the importance of this region as a Permian fossil Lagerstätte and inspired the Brazilian Government to create the Tocantins Fossil Trees Natural Monument (Dias-Brito et al., 2007). However, although the Parnaíba Basin received special attention during recent years, and several taxa have been described recently, the region's palaeophytogeographic setting remains poorly investigated. Based on the presence of *Psaronius* and the absence of *Glossopteris*, Dolianiti (1972) suggested an affinity with Europe and North America. Based on the presence of *Arthropitys*, *Amyelon*, and *Artisia*, Coimbra and Mussa (1984) and Mussa and Coimbra (1987) suggested an affiliation to the Euramerican Province but, on the other hand, the presence of *Taxopitys* suggests an affiliation to Gondwana. Rößler and Galtier (2002a) described *Grammatopteris freitasii* from this basin, a genus otherwise restricted to France and Germany, but with close relations to the filicalean *Rastropteris* from Cathaysia (Galtier et al., 2001). More recently, Kurzawe et al. (2013b) identified *Damudoxylon*, *Taeniopitys* and *Kaokoxylon* in the Parnaíba Basin – all genera typically from Gondwana.

In this second contribution we continue describing arboreal sphenophytes introducing two additional species, *Arthropitys tocantinensis* sp. nov. and *Arthropitys barthelii* sp. nov., and we initiate a discussion concerning the palaeophytogeographic position of the Parnaíba Basin during the Cisuralian.

2. Material and methods

The specimens were found in the southern part of the Parnaíba Basin, between Filadélfia and Araguaína cities, State of Tocantins, central-north Brazil (Fig. 1). In order to investigate the morphological and internal structure of the petrified specimens, we used a sand blaster to remove the psammitic sediment and expose the surface. The specimens were subsequently cut with a trimming saw to reveal both transverse and longitudinal (radial and tangential) sections. These surfaces were ground and polished applying standard procedures. Cellular structures were examined and photographed under reflected light using a Nikon DS-5M-L1 digital camera attached to Nikon Eclipse ME 600 and Nikon SMZ 1500 microscopes. Morphological overviews were photographed with a Nikon D 200 camera; larger polished surfaces were digitalised using an Epson Perfection V330 scanner. Composite images were created using Corel Draw version X6 and corrected only for contrast and colour. The specimens are stored in the Museum für Naturkunde, Chemnitz, Germany, labelled as K 4965, K 5266, K 5399, K 5455, K 5456, K 5787, K 5500, K 4874, and K 6040. The paleophytogeographical analysis and the Jaccard Coefficient were ascertained using PAST (Hammer et al., 2001).

3. Systematic paleontology

Class Sphenopsida
Order Calamitales
Family Calamitaceae
Genus: *Arthropitys* Goeppert, 1864–1865
Type-species: *Arthropitys bistriata* (Cotta) Goeppert *emend*. Rößler et al., 2012

Arthropitys tocantinensis sp. nov. Neregato, Rößler et Noll
Holotype: K 4965.
Paratype: K 5266.
Additional material: K 5399, K 5455, K 5456.
Type locality: Northern Tocantins Petrified Forest, Tocantins State, Parnaíba Basin, central-north Brazil.
Type stratum: Motuca Formation, Permian.
Etymology: The specific name refers to the State from which this species was identified Tocantins, central-north Brazil.
Diagnosis: Branching system composed of variable number (mostly 3–12) of branches occurring at every node, superposed or alternating along the stem, with and without secondary growth. Segmentation of fascicular wedges and interfascicular rays only visible within the proximal wood. Secondary xylem tracheids with exclusively scalariform pitting. Ray parenchyma with pitted horizontal walls.
Description
General features and taphonomy – The holotype, K 4965, an erosional remnant of a petrified trunk represents the basal portion of a branched woody stem (Plate I, 1). The specimen was found embedded in well-rounded, well-sorted, and medium-grained fluvial quartz sandstone (grain size: 293 [140–670] μm), not always easily removable from the stem; in some cases the adhering sandstone is also strongly silicified up to 40 mm from the axis. The stem surface is partially eroded depending on the extent of silicification, therefore no extraxylary tissues are preserved. The stem base is enlarged, probably forming a woody root stock with obliquely downwardly oriented woody projections and scars (Plate I, 1, lower part). However, the eroded stem surface prohibits to recognise further morphological detail. At the top of the specimen, woody branches indicate a three-dimensional branching architecture. The two woody branches, probably originating from the bifurcation of the stem, measure 26 × 44 mm and 63 × 90 mm in diameter, with the longest including an angle with the uppermost stem of 55°. The stem portion is 1850 mm long with its largest width at the base of 130 × 213 mm, girth of 554 mm; the pith cavity at the base measures 2 × 9 mm. Above 260 mm the base, stem diameter measures 90 × 119 mm, pith cavity is 7.5 × 13.5 mm wide and girth is 448 mm (Plate I, 4). Beneath 350 mm of the upper end, the stem diameter measures 95 × 105 mm (Plate I, 3); At the top, the stem diameter measures 52 × 62 mm, pith cavity is 9 × 20 mm and girth is 180 mm (Plate I, 2). Largest pith cavity diameter of 19 × 25.5 mm occurs 530 mm from the upper end of the stem portion. Nodes are barely visible on the stem's surface; on one radial section (Plate II, 1) internode length is 63 mm.

The paratype, K 5266, represents a branched stem portion from the upper tree (crown position) likewise partly embedded in medium-grained quartz sandstone. The specimen is 1170 mm long and bears numerous closely spaced nodes with internode lengths at the lower end of

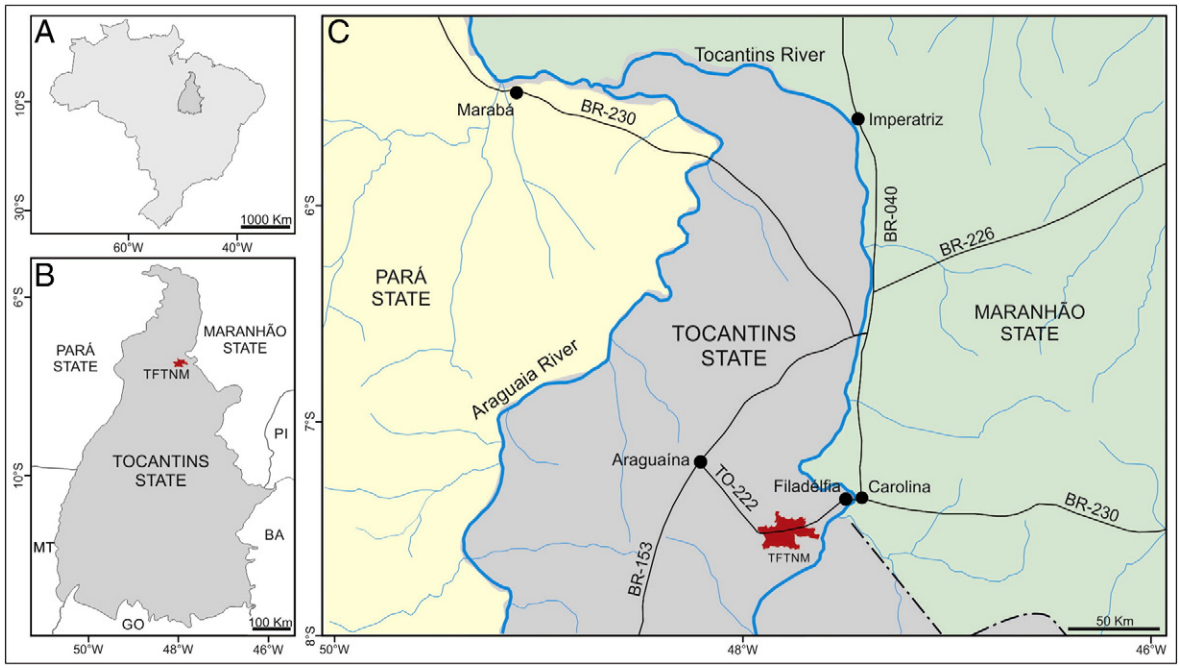

Fig. 1. A: Map of Brazil with the position of Tocantins State. B: Map of Tocantins State with the localization of the Tocantins Fossil Trees Natural Monument (TFTNM). MT: Mato Grosso State; GO: Goiás State; BA: Bahia State; PI: Piauí State. C: Detailed map of the North of Tocantins State showing the position of the Tocantins Fossil Trees Natural Monument and the most important municipalities around it.

12–20 mm, and at the upper end of 9–12 mm (Plate III, 1–2; Plate IV, 2–3). The stem diameter at the lower end is 87 mm, and at the upper end 65 mm. Pith cavity diameter is approximately 15 mm at the lower end diminishing to 8 mm at the upper end.

K 5456 (Plate V, 1) represents a stem/branch portion, 276 mm long. The diameter at the lower end is 35 × 38 mm, pith cavity spans 13 × 14 mm surrounded by 62 vascular strands (Plate V, 5, 8), presenting asymmetric secondary body (Plate V, 4). At the upper end, the stem diameter is 36 × 44 mm, pith cavity spans 12 × 13 mm and is surrounded by 62 vascular strands (Plate V, 2). Eleven nodes are visible (counted from three portions belonging to the specimen), internode distances are 27 (15–36) mm (Plate V, 1); several nodes show branch traces (up to 10 visible). Additionally, two large branch traces, 11 × 13 mm and 24 × 26 mm in diameter and showing extended secondary growth, are visible at the stem surface (Plate V, 1).

K 5455 (Plate V, 6, 7) is an erosional remnant of a stem, 198 mm long, 69 × 85 mm in diameter. The pith cavity is asymmetric, 15 × 19 mm in diameter and surrounded by approximately 80 vascular strands. Three nodes are visible on the surface bearing several branch traces, which in some cases became overgrown during secondary growth of the stem. A few of the side branches enlarged during secondary growth to form woody branches (WB in Plate V, 6), one is visible in this specimen.

K 5399 is a stem portion 170 mm long, 76 × 88 mm in diameter with a pith cavity of 9 × 11 mm surrounded by 68 vascular segments. Two woody branch scars are present, one hidden below the sandstone cover, another measuring 8 × 10 mm. Nodes are not visible on the outer stem surface, one additional branch scar measures approximately 7 × 7 mm. The transverse section reveals several "growth interruptions", which are also visible on the eroded surface.

K 5400 is another stem portion, cut obliquely at an angle of ca 35° to the stem axis. The transverse section shows distinct "growth interruptions", also accentuated on the eroded surface. Two nodes are recognisable separated by. ca 50 mm and bear several branch traces, 6–16 mm in diameter. Although quite similar in overall appearance to K 5266 and K 5455, there is insufficient evidence to assign the material to one plant.

Branching system – The branching system in this species is characterised by (1) woody branches originating from secondary growth of single side branches or bifurcations of the stem forming a three-dimensionally projecting crown, and (2) by side branches departing from the nodes. These side branches can occur at every node, but usually are of variable number per node, 3–12 in the present material. Side branches are recognisable as branch scars at the outer stem surface (Plate III, 1–3) or as branch traces in tangential sections (Plate II, 1–3, 6–7; Plate III, 4). Secondary growth can be present or absent in these traces or scars; in some cases individual branch traces became overgrown during stem thickening. In K 4965, branch traces/scars are elliptical averaging 5.19 (4.78–5.54) mm in height and 3.54 (2.66–4.13) mm in width (Plate II, 1–3, 6–7).

K 5266 shows three woody branches departing from the stem and probably originating from successive bifurcations of the stem, whereupon the upright stem maintained dominance. The lowermost one, 105 mm distant from the lower end, is 196 mm long and 36 × 38 mm in diameter, having a small pith cavity of 4 mm diameter and likewise several nodes carrying abundant small branch scars. The second one, 525 mm above the lower end of the specimen, is 50 mm long and 22 mm in diameter. The third branch, 1125 mm from the lower end, is ca 30 mm long and 32 mm in diameter. Additionally, K 5266 bears numerous irregular positioned branch scars or traces of variable size reaching 2–27 mm in diameter (Plate III, 1–6; Plate IV, 1–2, 4, 6–7).

Anatomy of primary tissues – Carinal canals in K 4965 are elliptical averaging 290 (180–420) μm radially and 210 (140–290) μm tangentially, and are surrounded by several rows of circular to polygonal metaxylem elements, 49 (13–120) μm in diameter (Plate I, 6), with annular thickenings (Plate II, 4). In K 5266, carinal canals are collapsed; surrounding metaxylem elements average 39 μm (20–54) in diameter (Plate III, 7).

Anatomy of secondary tissues – In transverse section, a clear distinction between interfascicular rays and fascicular wedges is only visible within the innermost wood (Plate I, 7; Plate III, 7); it becomes less obvious more distally (Plate I, 5; Plate III, 5). However, in longitudinal tangential section the segmentation of the secondary body is still recognisable and continues from node to node (Plate II, 7; Plate IV, 4).

Nevertheless, in the description chart, ray parenchyma is characterised without any assignment to interfascicular or fascicular rays.

In K 4965, wood thickness ranges between 25 and 89 mm. At the base, and 300 mm above the base, the secondary body consists of 55 primary vascular bundles or fascicular wedges (Plate I, 4: section A); 1470 mm above the base, 76 fascicular wedges are recognisable (Plate I, 3: section B); and at the top of the stem portion, 84 fascicular wedges surround the pith (Plate I, 2: section C), revealing part of the epidogenetic phase of the plant development. In transverse section, interfascicular rays and fascicular wedges are clearly distinguishable up to 10–15 mm from the pith periphery (Plate I, 6; Plate III, 7), because tracheid files became intercalated in the proximal interfascicular rays very early in ontogenetic development (Plate I, 7). In the innermost wood, fascicular wedges are composed of up to 27 cell files averaging 0.69 (0.45–0.88) mm in width. Tracheids are square to rectangular averaging initially 41 (30–70) μm radially and 30 (22–50) μm tangentially, in the distal wood 55 (40–70) μm radially and 46 (20–70) μm tangentially (Plate I, 5). Rays are composed of 3–10 parenchyma rows, 204 (100–340) μm wide in the inner wood with rectangular cells averaging 135 (50–210) μm radially and 31 (18–70) μm tangentially (Plate I, 6–7), and in the outer wood rays averaging 292 (190–520) in width. In both K 4965 and K 5266, ray parenchyma cells commonly bear circular pits in the horizontal walls (Plate II, 5; Plate IV, 5), although pristine anatomical preservation is required to recognise this character.

K 5266 has a maximum wood thickness of 36 mm, several growth-ring-like concentric tissue density variations are recognisable throughout the wood (Plate III, 5–6).

In radial section, secondary xylem tracheids have exclusively scalariform pitting in their radial walls (Plate II, 4; Plate IV, 8). In K 4965, 16 pits occur per 100 μm vertical distance (Plate II, 4). Interfascicular rays are composed of rectangular parenchymatous cells, averaging 89 (50–170) μm axially and 108 (73–140) μm radially.

In tangential section, the high portion of parenchyma is most conspicuous, with the secondary body composed of at least 35% of parenchyma (Plate II, 7; Plate IV, 4). In K 4965, tracheids are several millimetres long. Parenchymatous cells of interfascicular rays average 70 (30–170) μm axially and 39 μm (10–70) μm tangentially.

Leaf traces – In nodal position, closely beneath the branch traces, small elliptical leaf traces were recognised. They measure 1.36 (1.11–1.61) mm in height and 0.43 (0.29–0.56) mm in width (Plate II, 6–7; Plate IV, 4; Plate V, 3, 9).

Extraxylary, cortical tissues and periderm – Due to transport abrasion the external surface of the specimens lacks any extraxylary tissues.

Arthropitys barthelii sp. nov. Neregato, Rößler et Noll

Holotype: K 5787.

Additional material: K 4874, K 5500, K 6040.

Type locality: Tocantins Fossil Trees Natural Monument (TFTNM), Parnaíba Basin, central-north Brazil.

Type stratum: Motuca Formation, Permian.

Plate I. *Arthropitys tocantinensis* sp. nov., holotype K 4965.1: Gross morphology of the stem showing enlarged stem base with smallest pith (P), departing woody roots (R) and a trifurcated branching pattern with large woody branches (WB) at the top. Scale bar = 100 mm.2: Transverse section from the top of the specimen showing pith cavity and surrounding wood consisting of 84 fascicles. Scale bar = 10 mm.3: Transverse section from the middle part of the specimen showing pith cavity (PC) and 76 surrounding wood fascicles. Scale bar = 10 mm.4: Transverse section from close above the stem base showing small compacted pith cavity and surrounding wood consisting of 55 fascicles. Scale bar = 10 mm.5: Detail of transverse section of Fig. 3 showing the wood consisting of tracheid files and rays. Near the stem periphery there is no clear distinction between interfascicular rays and fascicular rays. Scale bar = 500 μm.6: Detail of transverse section of Fig. 3 showing initial fascicles and interfascicular rays (IR). Carinal canals (CC) are surrounded by several rows of circular to polygonal metaxylem elements (MX). Scale bar = 500 μm.7: Detail of transverse section of Fig. 3 showing initial fascicles and interfascicular rays (IR). Note the progressive inclusion of tracheid files (arrow) close to the pith margin leading to a rather homogeneous wood without clear segmentation. Scale bar = 200 μm.

Plate II. *Arthropitys tocantinensis* sp. nov., holotype K 4965.1: Radial section showing pith cavity (PC), wood and two nodes with branch traces (BT). Scale bar = 10 mm.2: Tangential section from the innermost wood showing two nodes (N), the lower with several branch traces (arrows). Note the clear segmentation in distinct fascicles. Scale bar = 10 mm.3: Tangential section from the median wood showing two nodes (N), the lower with branch traces (arrows). Note the weak segmentation of the wood with increasing distance from the pith. Scale bar = 10 mm.4: Radial section showing annular thickening of the metaxylem (MX) and scalariform pitting of the secondary xylem (SX). Scale bar = 100 μm.5: Transverse section showing tracheid files aligned to an interfascicular ray (IR). Note the pitting pattern of the ray cells (arrows). Scale bar = 100 μm.6: Detail of Fig. 2 showing branch traces (BT) close above the node, leaf traces (LT) in nodal position and clear segmentation of the wood. Scale bar = 2 mm.7: Detail of Fig. 3 showing branch traces (BT) close above the node and leaf traces (LT) in nodal position. Note the weak segmentation of the wood and the initial secondary growth of the branch trace. Scale bar = 2 mm. (see on page 42)

Plate III. *Arthropitys tocantinensis* sp. nov., paratype K 5266.1: Two aspects of the stem's gross morphology showing many small branch scars irregularly distributed over the surface and three large woody branches (WB). Scale bar = 100 mm.2: Stem surface showing irregularly distributed branch scars (arrows) at the nodes (N). Note the different size of branch scars. Scale bar = 10 mm.3: Stem surface showing one branch scar (arrow) with secondary growth and pith cavity. Scale bar = 10 mm.4: Tangential section of the stem showing several nodes (N) with different size branch traces (arrows) reflecting different developmental stages. Scale bar = 10 mm.5: Half transverse section of the stem (PC: pith cavity) in nodal position showing several branch traces (arrows) crossing radially the wood. Note the dense succession of concentric growth ring-like patterns. Scale bar = 10 mm.6: Detail of Fig. 5 showing the course of a branch trace. Scale bar = 2 mm.7: Detail of Fig. 5 showing the innermost wood still clearly segmented in fascicular wedges and interfascicular rays (IR). Scale bar = 200 μm. (see on page 43)

Plate IV. *Arthropitys tocantinensis* sp. nov., paratype K 5266.1: Stem surface showing a abruptly enlarging branch scar. Scale bar = 10 mm.2: Tangential section showing five successive nodes (N) with irregular distributed branch traces. Arrow indicates the branch trace of the large scar visible on Fig. 1. Scale bar = 10 mm.3: Radial section showing pith cavity with five nodes. Scale bar = 10 mm.4: Tangential section showing two nodes (N) with several leaf traces (LT) and slightly above the nodes a few branch traces (BT). Scale bar = 2 mm.5: Transverse section of the innermost wood showing an interfascicular ray (IR) with pitted parenchyma cells. Scale bar = 200 μm.6: Tangential section showing a branch trace with small amount of secondary growth. Scale bar = 1 mm.7: Tangential section showing a branch trace without secondary growth. Scale bar = 1 mm.8: Radial section showing pitting of the secondary xylem. Scale bar = 100 μm. (see on page 44)

Plate V. *Arthropitys tocantinensis* sp. nov., specimen K 5465, except 6 and 7, K 5455.1: Stem or branch portion showing several nodes (N) with irregularly positioned branch scars and two large woody branch scars (WB). Scale bar = 10 mm.2: Transverse section from the upper end of the stem portion showing pith cavity surrounded by 61 wood fascicles. Scale bar = 10 mm.3: Tangential section showing one node with leaf traces (LT) and slightly above several branch traces (BT). Scale bar = 10 mm.4: Radial section of the stem portion showing pith cavity with one node and asymmetric wood development. Scale bar = 10 mm.5: Transverse section from the lower end of the stem portion showing pith cavity surrounded by 62 wood fascicles. Scale bar = 10 mm.6: Erosional remnant of K 5455 showing three nodes (N) with several branch scars and one large woody branch (WB). Scale bar = 10 mm.7: Transverse section of K 5455 with pith and surrounding wood. Note the rhythmic pattern of the secondary growth. Scale bar = 10 mm.8: Detail of Fig. 5 showing two fascicular wedges and interfascicular rays (IR) of the innermost wood. Scale bar = 500 μm.9: Detail of Fig. 3 showing leaf traces (LT) in nodal position and slightly above positioned branch traces (BT). Scale bar = 1 mm. (see on page 45)

Plate VI. *Arthropitys barthelii* sp. nov., holotype K 5787.1: Basal stem portion showing several nodes with irregularly positioned branch scars (red dots). Scale bar = 50 mm.2: Transverse section from the upper end of the stem showing deformed pith cavity. Note the very homogeneous appearance of the wood. Scale bar = 10 mm.3: Transverse section 163 mm above the lower end of the stem showing small pith cavity surrounded by 28 vascular segments. Note the very homogeneous appearance of the wood. Scale bar = 10 mm.4: Eroded bottom surface of the stem showing the pith cavity (PC) and eight roots (arrows) emerging from five different nodes. Scale bar = 10 mm.5: Detail of Fig. 2 showing a proximal vascular segment with carinal canal (CC), metaxylem (MX) and secondary xylem (SX). Scale bar = 100 μm.6: Detail of Fig. 3 close to pith cavity showing several proximal vascular segments with carinal canal (CC) and between them interfascicular rays (IR). Scale bar = 200 μm.7: Detail of Fig. 2 showing the outer wood made of tracheid files and parenchymatous rays. Scale bar = 100 μm.8: Ray parenchyma showing small circular pits (arrows) in their horizontal walls. Scale bar = 100 μm. (see on page 46)

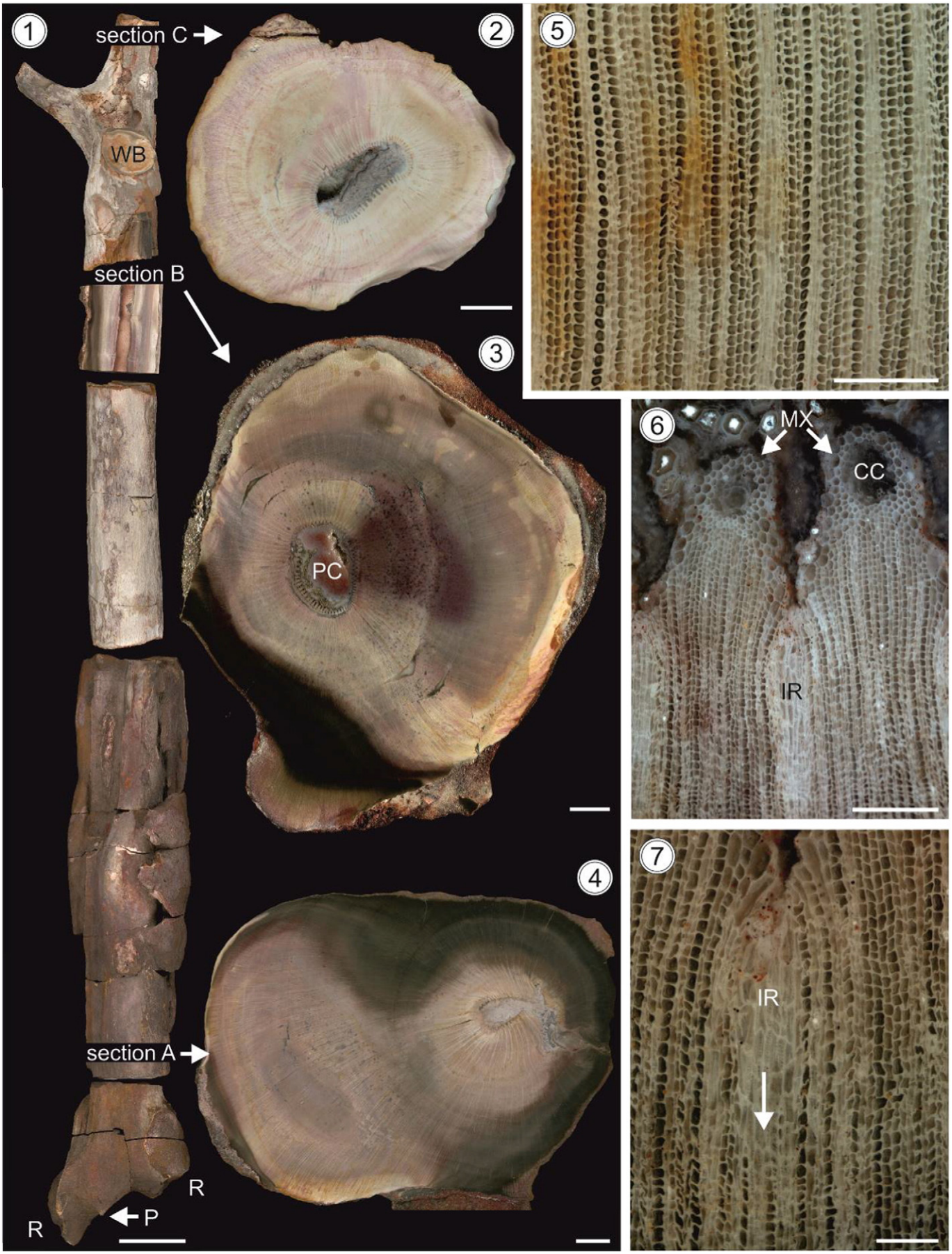

Plate I.

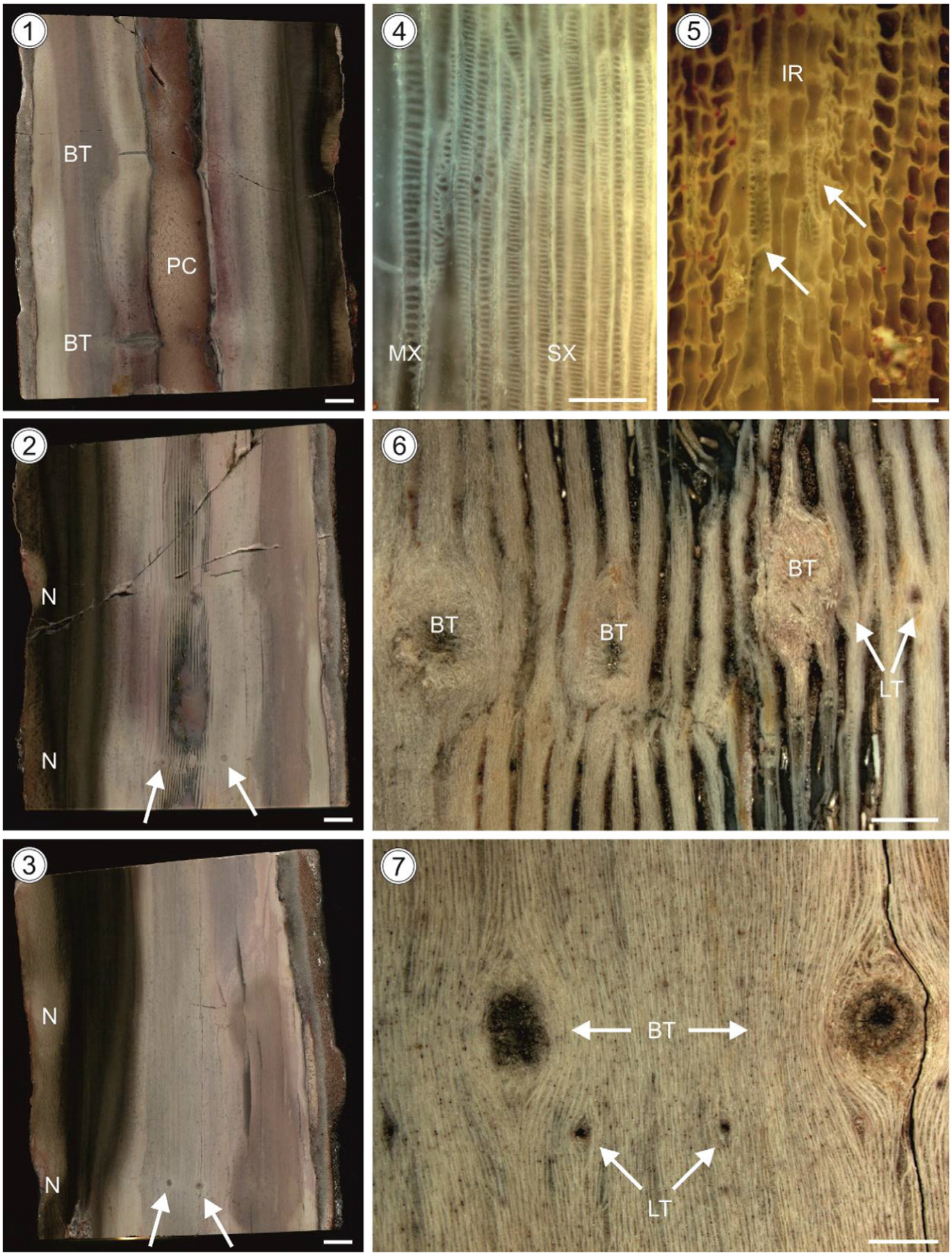

Plate II (*caption on page 40*).

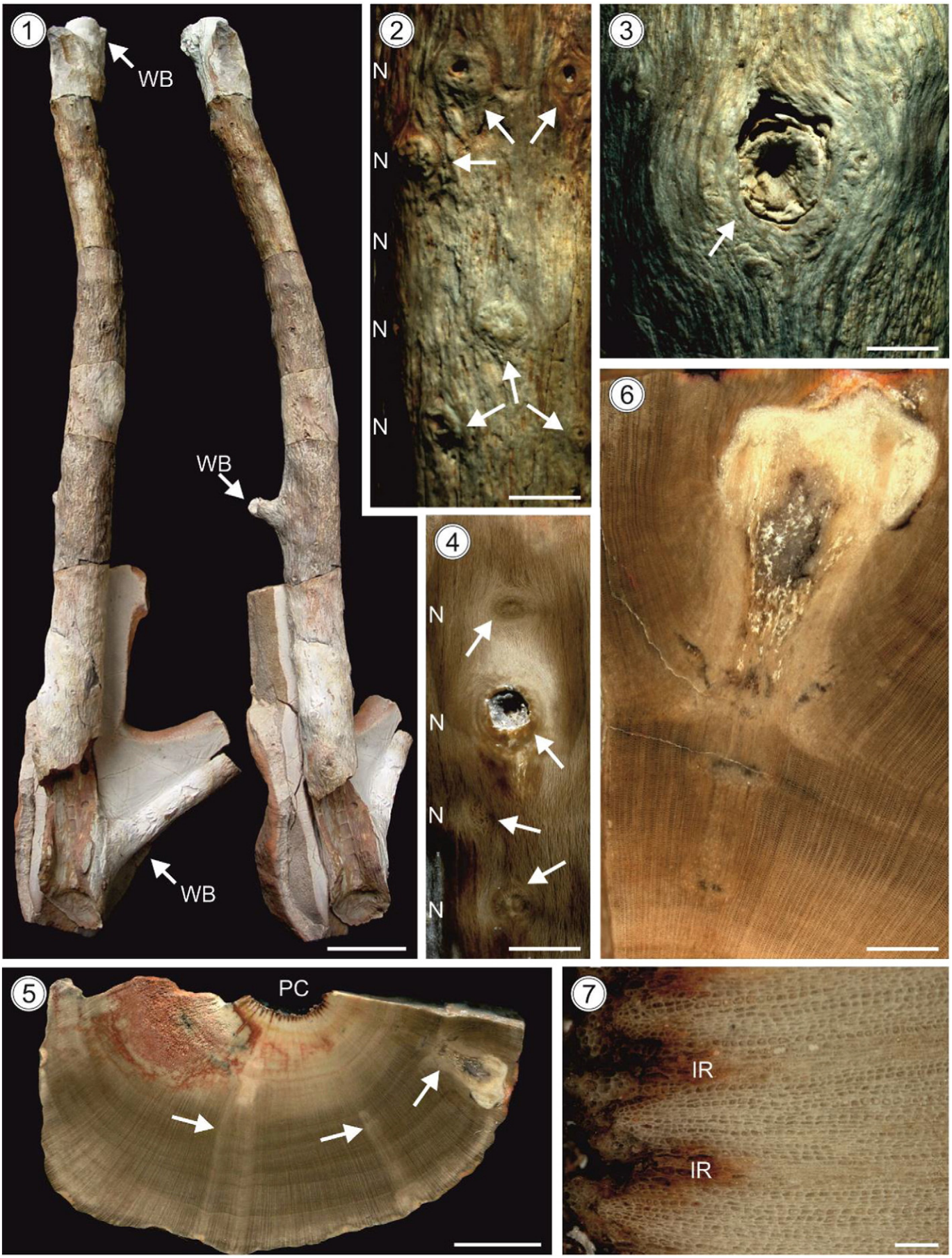

Plate III (*caption on page 40*).

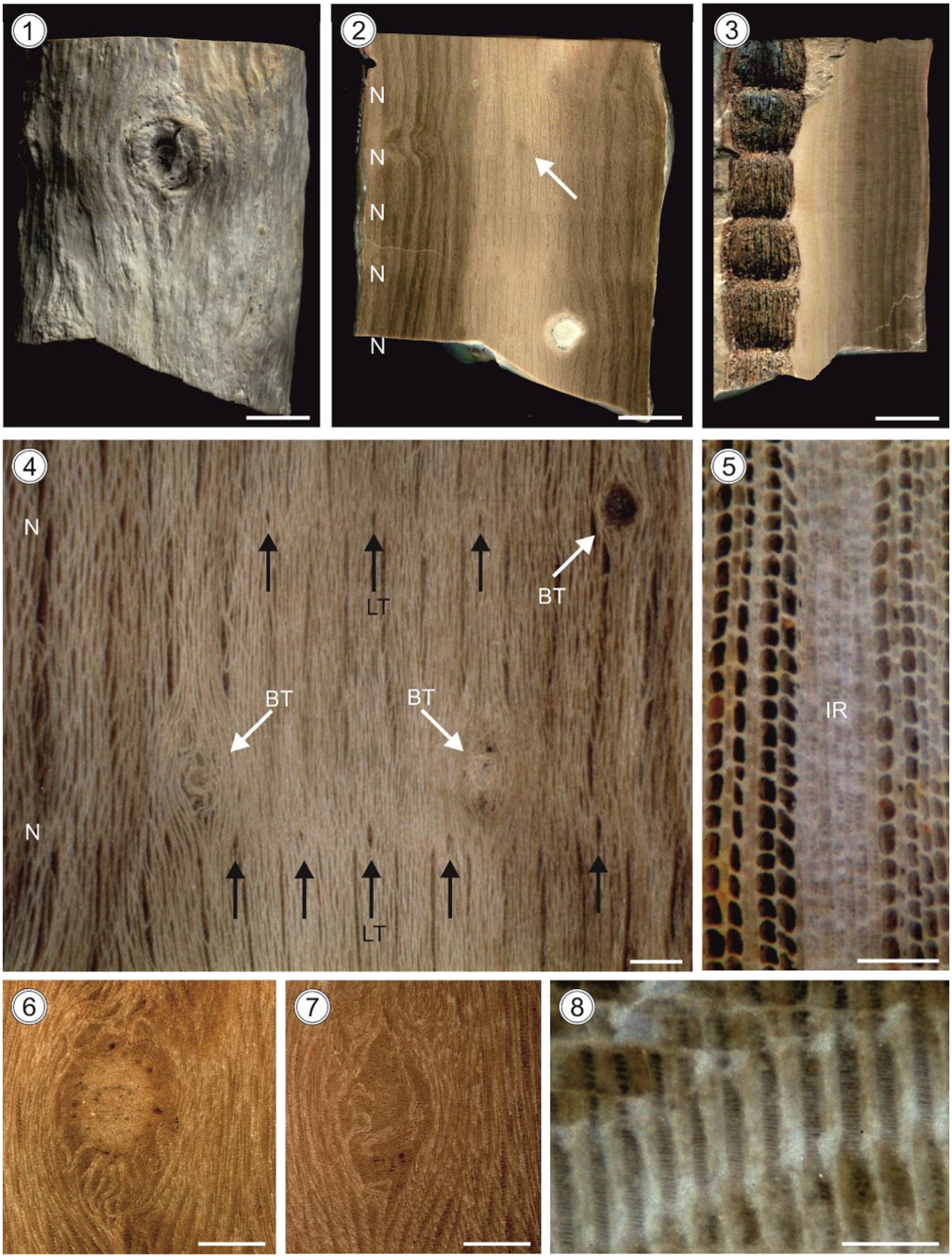

Plate IV (*caption on page 40*).

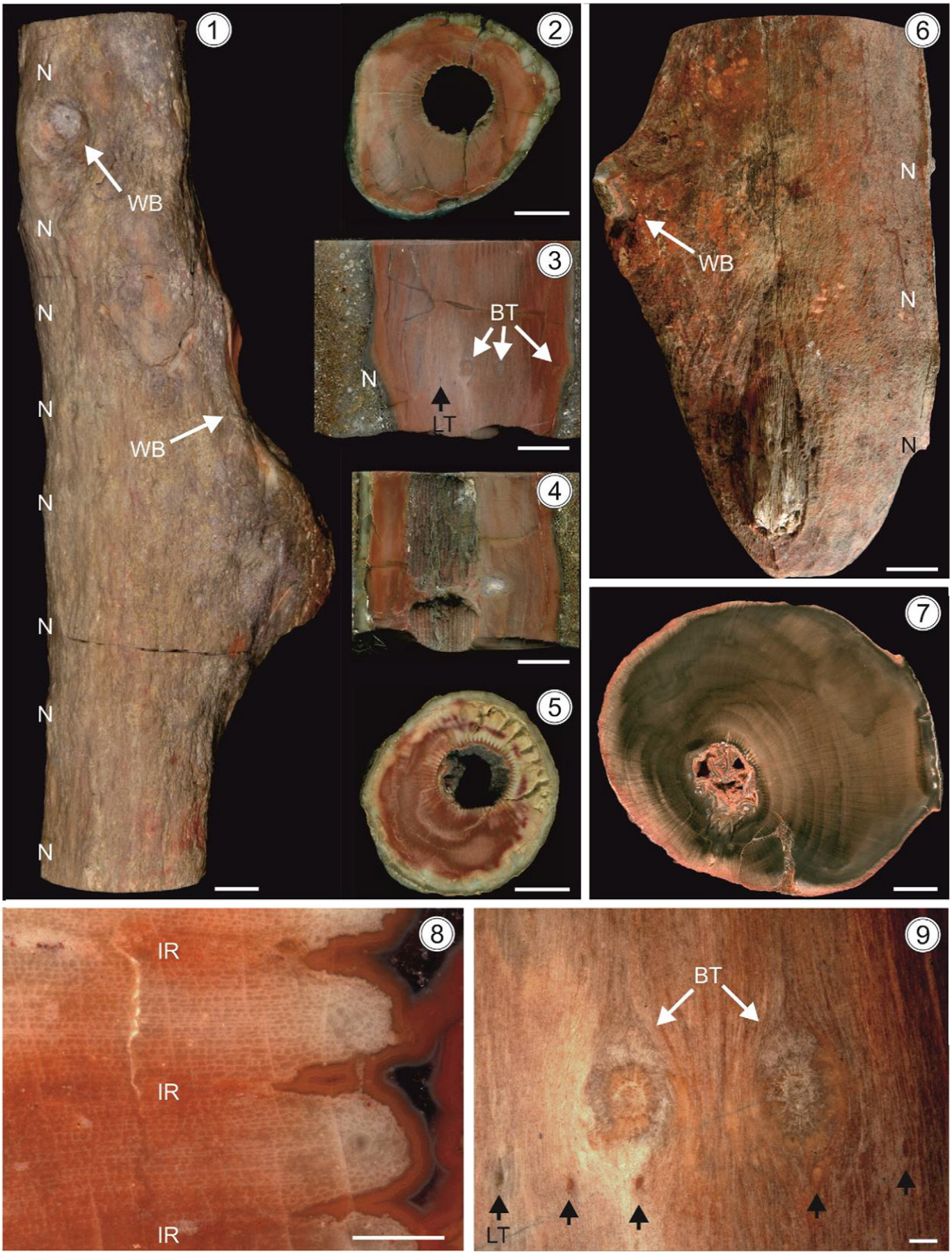

Plate V (*caption on page 40*).

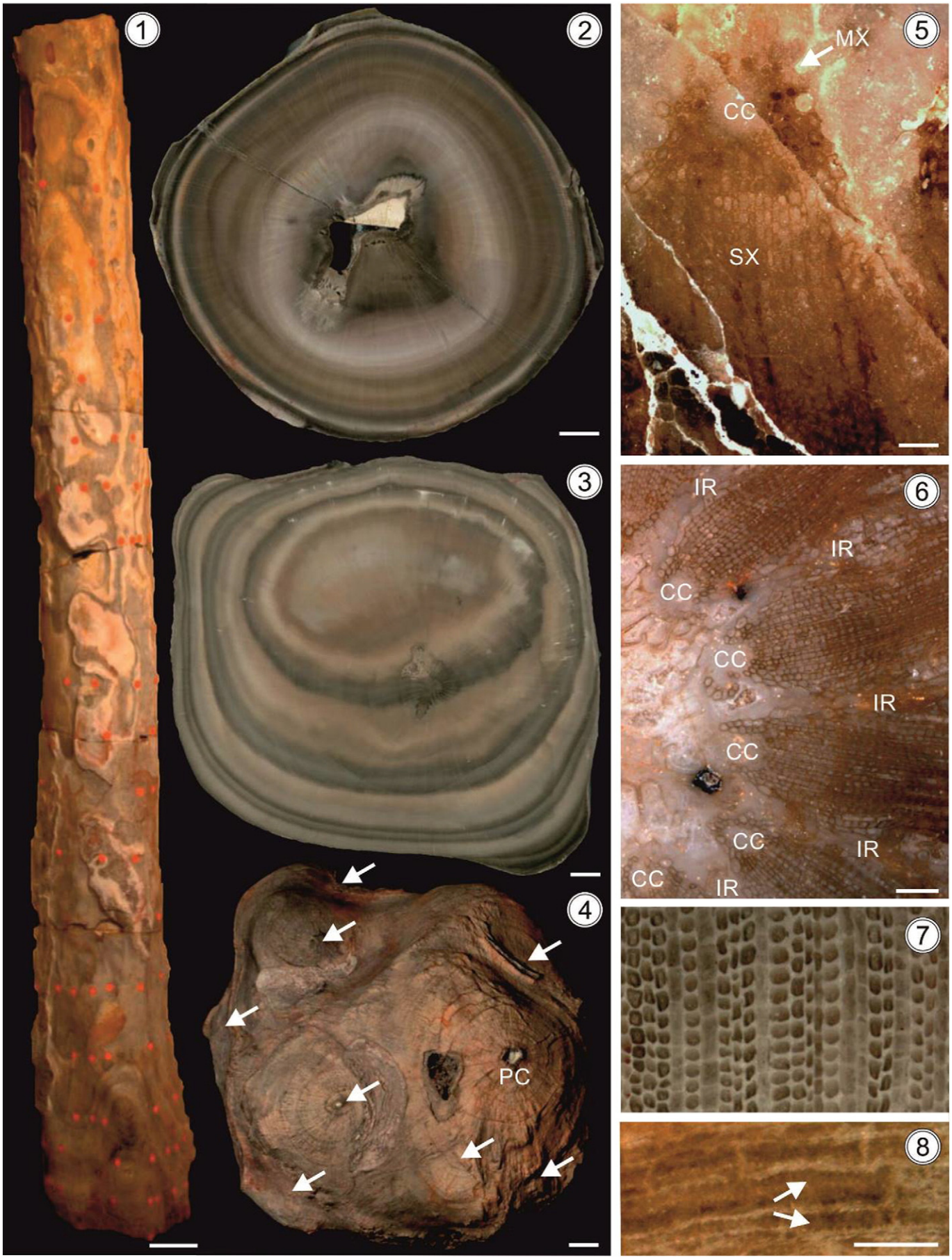

Plate VI (*caption on page 40*).

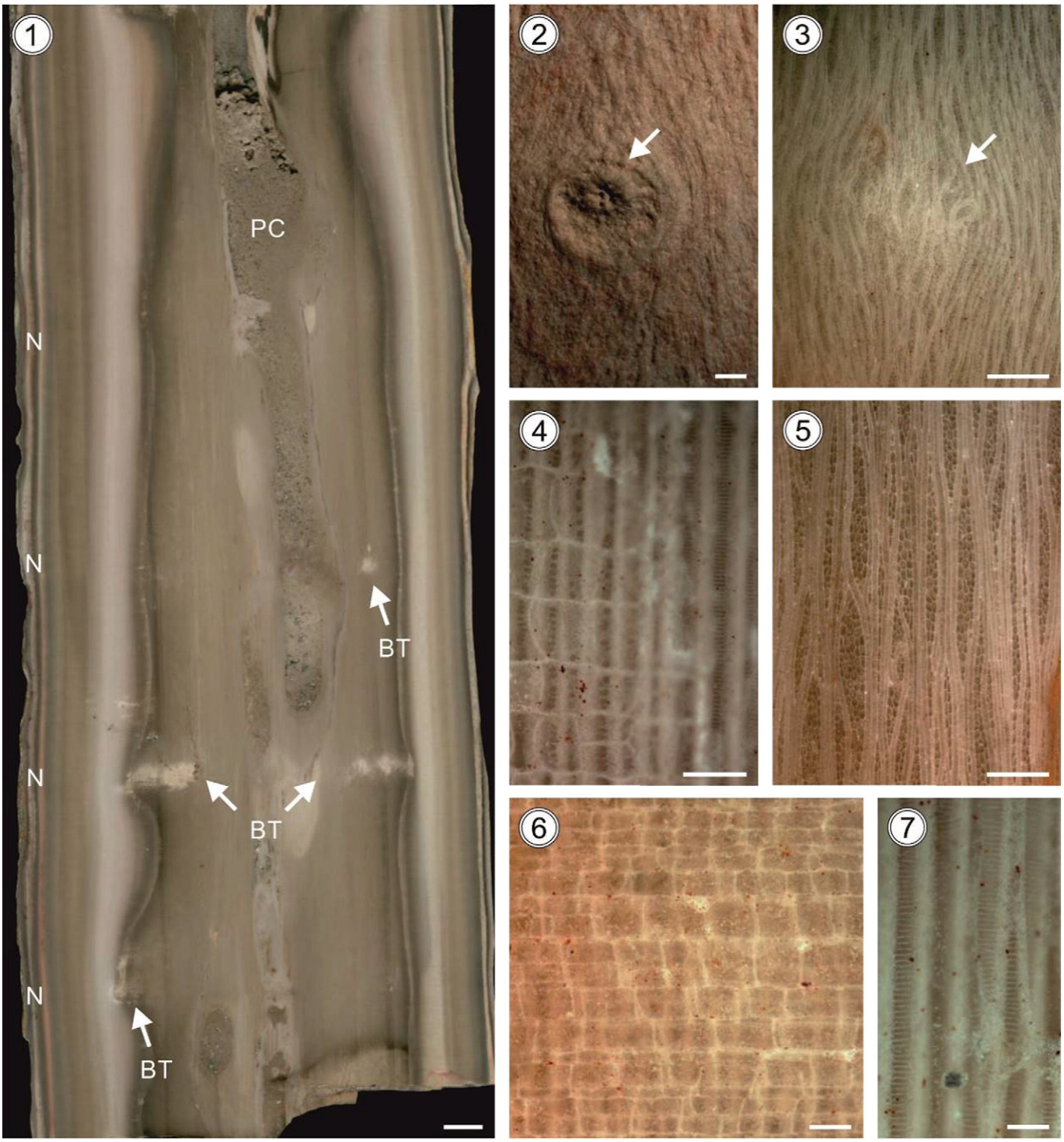

Plate VII. *Arthropitys barthelii* sp. nov., holotype K 5787. 1: Radial section from the upper part of the stem portion showing several nodes (N) with weak branch traces (BT) and an irregular pith cavity probably affected by boring (PC). Scale bar = 10 mm. 2: Outer surface of the stem showing a branch scar (arrow). Scale bar = 1 mm. 3: Tangential section of the stem showing a branch trace (arrow) without any secondary growth. Scale bar = 1 mm. 4: Radial section showing scalariform pitting of the secondary xylem tracheids (right) and variable crossfield pitting (left). Scale bar = 100 μm. 5: Tangential section showing parenchyma-rich wood without any distinction of interfascicular or fascicular rays. Scale bar = 500 μm. 6: Radial section showing brick-shaped cells of a parenchymatous ray. Scale bar = 100 μm. 7: Radial section showing scalariform pitting of the secondary xylem. Scale bar = 50 μm.

Etymology: The specific name is dedicated to our friend, palaeobotanist Prof. Dr. Manfred Barthel, Berlin, in recognition of his encouraging work on late Paleozoic floras and terrestrial ecosystems in general.

Diagnosis: This species presents 2–17 side branches at every node; side branches lack secondary growth and are disposed in irregular pattern. Homogeneous wood without distinct interfascicular rays and fascicular wedges, except within the first few millimetres of the secondary body. Secondary xylem tracheids have only scalariform pitting. Circular to broad-oval pitting is present in crossfield areas. Ray parenchyma with pitted horizontal walls. 1–3 irregularly arranged first-order roots depart from the lowermost nodes and show secondary growth.

Remarks: Although pith diameters usually change during the ontogenetic development of the plant and are therefore regarded as of

minor diagnostic value, it is striking that the pith cavity in this species is very narrow in all investigated specimens irrespective of the amount of secondary growth. However, only in one case can we prove that a specimen is a lower stem portion based on the presence of root scars.

Description

General morphology – The holotype, K 5787, represents a portion of a basal stem, 1280 mm long, found as an abraided remnant in well-rounded, well-sorted, medium-grained quartz sandstone (Plate VI, 1). The stem's basal diameter is 150 × 180 mm; girth is 502 mm; slightly tapering upward and the enlarged base of the trunk has a pith cavity of 2.8 × 4.8 mm surrounded by 25 vascular segments; 88 mm distant from the lower end, the pith is surrounded by 28 vascular segments; at 163 mm above the lower end, the pith cavity is surrounded by 28 vascular segments (Plate VI, 3). At the upper end, the stem measures 104 × 114 mm, girth of 340 mm with a deformed pith cavity (Plate VI, 2). The ratio between pith cavity and stem diameter along the stem equals 1:15–30. The mean internode length is 57 (40–80 mm; n = 21).

Root system – The root system is composed of eight circular to oval first-order roots emerging vertically to slightly obliquely downward from several basal nodes; one from the lowermost node, three from the second node, two from the fourth node, one from the fifth node and one from the seventh node above the base (Rößler et al., 2014) (Plate VI, 4). Although nodes three and six bear several mm-size scars, no woody roots are preserved. Other nodes also bear several additional mm-sized scars, e.g., node number four hosts 23 additional scars. The distance between the lowermost node to the seventh node is 25 cm. From the eighth node upward, only mm-size scars are recognisable, which may represent scars of former side branches (leafy twigs). The lowermost internodes are 30–35 mm apart. Above the sixth node, internodes increase gradually in length. The roots measure 30–52 mm in diameter and contain considerable secondary xylem surrounding small circular piths. Growth-ring-like concentric density variations of the secondary xylem are visible both in the trunk wood (Plate IX, 3) and in the roots (Plate VI, 4) and may denote seasonal changes in the environment. In these levels, the wood tracheids have reduced diameters, but the parenchymatous cells of the rays remain not only unaffected, they broaden slightly.

Branching system – In this species, the branching system is very distinct, 2–17 branches per node have been recognised, usually occurring at every node, without any secondary growth, irregularly distributed (Plate VI, 1). Branch traces/scars point to small and delicate side branches (Plate VII, 2; Plate VIII, 3), in some cases overgrown during stem enlargement and, therefore, indistinct on the stem surface or on the radial/tangential section (Plate VII, 1, 3; Plate VIII, 1). Minimum tangential distance between neighbouring branch traces is 14 mm.

Anatomy of primary tissues – In K 5787, carinal canals reach 160 (120–210) μm radially and 140 (100–170) μm tangentially, surrounded by circular to polygonal metaxylem elements averaging 34 (10–70) μm in diameter (Plate VI, 5, 6). A conspicuous character is the very small pith, which not significantly enlarges upwards (Plate VI, 2, 3; Plate VIII, 2).

Anatomy of secondary tissues – The secondary body – quite unusual for calamitaleans – is characterised by a conspicuous homogeneous appearance. Rays become crowded very early between tracheid files to form a rather loose homogeneous wood (Plate VI, 2, 3; Plate VIII, 2). A few millimetres centrifugally from the primary tissues, a clear differentiation between interfascicular rays and fascicular wedges is not possible (Plate VII, 5; Plate VIII, 7), even in tangential section. Nevertheless, weak growth interruptions recognised in transverse section point to some kind of seasonality in the environment.

In K 5787, the secondary body ranges is 42–104 mm thick. The innermost wood fascicles consist of 1–3 tracheid rows and 1–3 intermediary parenchymatous rays averaging 0.48 (0.32–0.74) mm (Plate VI, 5, 6). In the innermost wood, tracheids are circular to rectangular, reaching 45 (30–68) μm radially and 37 (15–45) μm tangentially. In the median wood, tracheids average 55 (47–69) μm radially and 46 (35–60) μm tangentially. In the outer wood, 1–7 joint tracheid rows are evident confined by rays (Plate VI, 7). Interfascicular rays, only visible in the innermost part, measure 201 (100–420) μm in width and consist of 1–6 rectangular parenchymatous cells reaching 102 (55–220) μm radially and 40 (20–85) μm tangentially. Parenchymatous cells are pitted in their horizontal walls (Plate VI, 8).

Secondary xylem tracheids have exclusively scalariform pitting with 11–16 pits per 100 μm (Plate VII, 4, 7; Plate VIII, 5). Thickenings fork sporadically, especially close to the tracheid termini. Circular to broadly oval irregular pitting with 5–9 pits per 100 μm is present in crossfield areas (Plate VII, 4; Plate VIII, 6). In K 5787, tracheids measure several millimetres in length. Rays consist of brick-shaped parenchymatous cells, reaching 92 (50–220) μm axially and 109 (65–220) μm radially (Plate VII, 6).

In tangential section, the secondary wood mass is composed of approximately 40% parenchyma (Plate VII, 5; Plate VIII, 7). In K 5787, parenchymatous cells of the interfascicular rays (only innermost wood) are rectangular and measure 84 (40–130) μm axially and 43 (20–70) μm tangentially (Plate VII, 5).

Extraxylary cortical tissues and periderm are not preserved.

Additional material – K 5550 is a stem portion, 138 mm long, 102 × 120 mm in diameter, pith not completely preserved but approximately 3 mm in diameter (Plate VIII, 2). Nodes and branch scars are barely visible at the stem surface; in tangential view, one branch trace lacking secondary growth is recognisable (Plate VIII, 3). Secondary xylem has scalariform pitting (Plate VIII, 5) and variable broadly oval crossfield pitting (Plate VIII, 6). The wood is very homogeneous and parenchyma-rich; vascular segments only visible a few millimetres distally of the internal wood. Because it is not possible to differentiate interfascicular rays and fascicular rays, both are designated as parenchymatous rays (Plate VIII, 4, 7).

K 6040 is represented by one slice of a stem 11 mm thick and 116 mm in maximum diameter; a cavity within the pith resulting from herbivore damage, since clusters of small coprolites are visible at the interface of the pith cavity/internal wood (Plate IX, 1–2). At least 30 *Sphenophyllum* axes of various ontogenetic stages (Plate IX, 4, 5) and many small roots have been preserved in the calamite interior. This interesting interaction was probably established after animal boring damage of the calamite providing a special microhabitat that sheltered the development of many *Sphenophyllum* axes. Preservation of the latter is quite detailed including primary and secondary vascular tissues, multilayered cortex, epidermal layer, attached leaves and roots

Plate VIII. *Arthropitys barthelii* sp. nov., additional material K 5550.1: Tangential section of a stem portion showing a small branch trace (BT). Scale bar = 10 mm.2: Transverse section from the upper end of the stem showing the few millimetres sized pith. Note the very homogeneous appearance of the wood. Scale bar = 10 mm.3: Detail of Fig. 1 showing a parenchymatous branch trace. Scale bar = 500 μm.4: Detail of Fig. 2 showing the outer wood made of variable tracheid files and parenchymatous rays. Scale bar = 500 μm.5: Radial section showing scalariform pitting of the secondary xylem. Scale bar = 100 μm.6: Radial section showing some crossfield pittings in the secondary xylem (arrows). Scale bar = 100 μm.7: Tangential section showing parenchyma-rich wood without any distinction of interfascicular rays and fascicular wedges. Scale bar = 500 μm.

Plate IX. *Arthropitys barthelii* sp. nov., additional material K 6040.1: Transverse section of a stem showing an unusual enlargement of the pith with at least 30 *Sphenophyllum* axes. Scale bar = 10 mm.2: Detail of Fig. 1 showing vascular wedges of the proximal wood separated by interfascicular rays (IR). Note the cut pith margin with coprolite clusters (arrows) and small intruded roots (R). Scale bar = 500 μm.3: Detail of Fig. 1 showing the homogeneous outer wood made of parenchymatous rays (PR) and tracheid files. Note the growth ring-like density variation in the wood (arrow) showing reduced tracheid diameters and broadening of the rays. Scale bar = 200 μm.4: Detail of Fig. 1 showing a juvenile *Sphenophyllum* axis with central triarch stele, a few secondary xylem tracheid files surrounding extraxylary tissues. Scale bar = 1 mm.5: Detail of Fig. 1 showing a developed *Sphenophyllum* axis with central triarch stele with secondary growth (SX) and surrounding extraxylary tissues. Scale bar = 1 mm.6: Detail of Fig. 1 showing the margin of a *Sphenophyllum* axis with inner parenchymatous cortex (CP), an outer sclerenchymatous cortex (CS) and an attached leaf (arrow). Scale bar = 500 μm. (see on page 50)

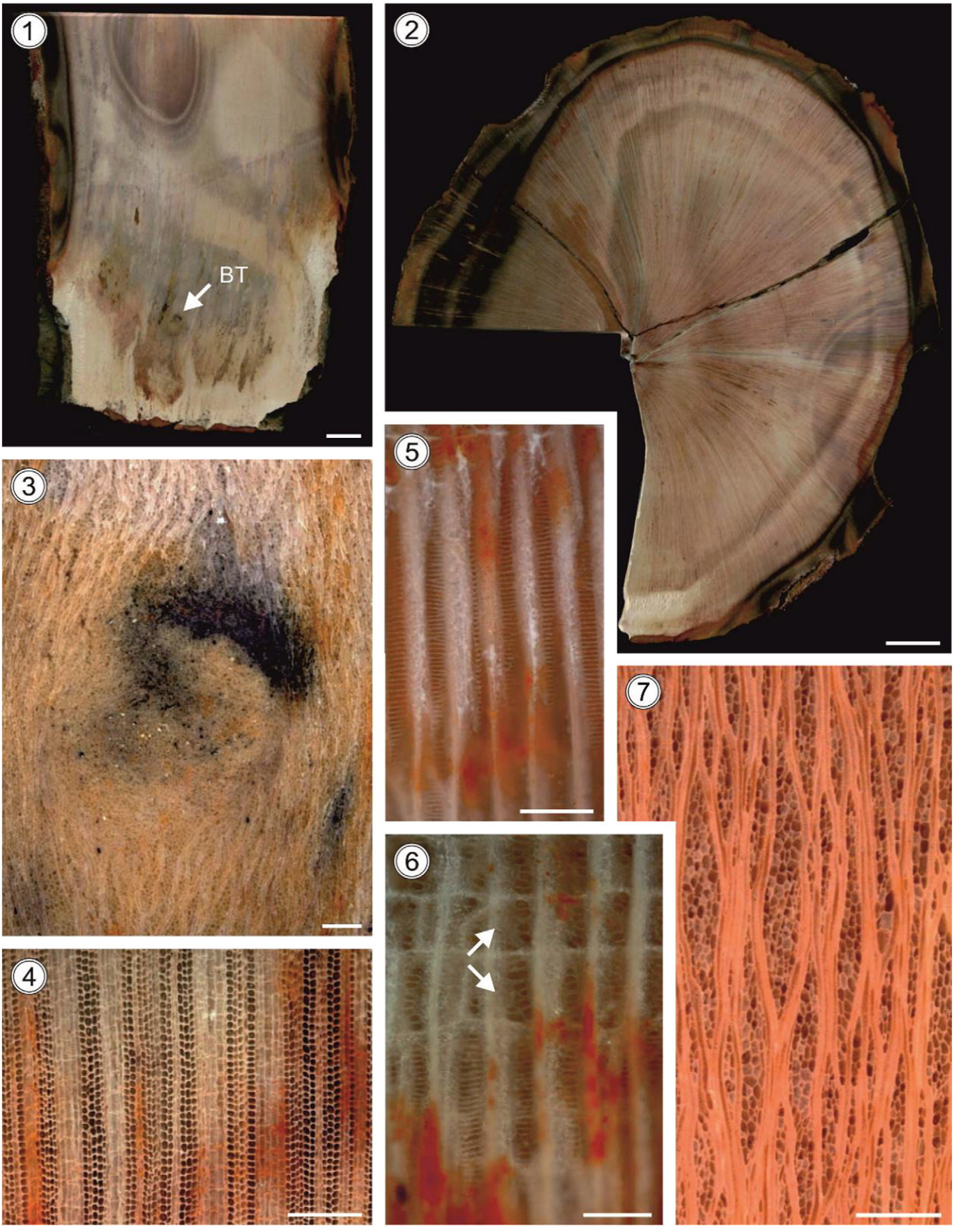

Plate VIII (*caption on page 48*).

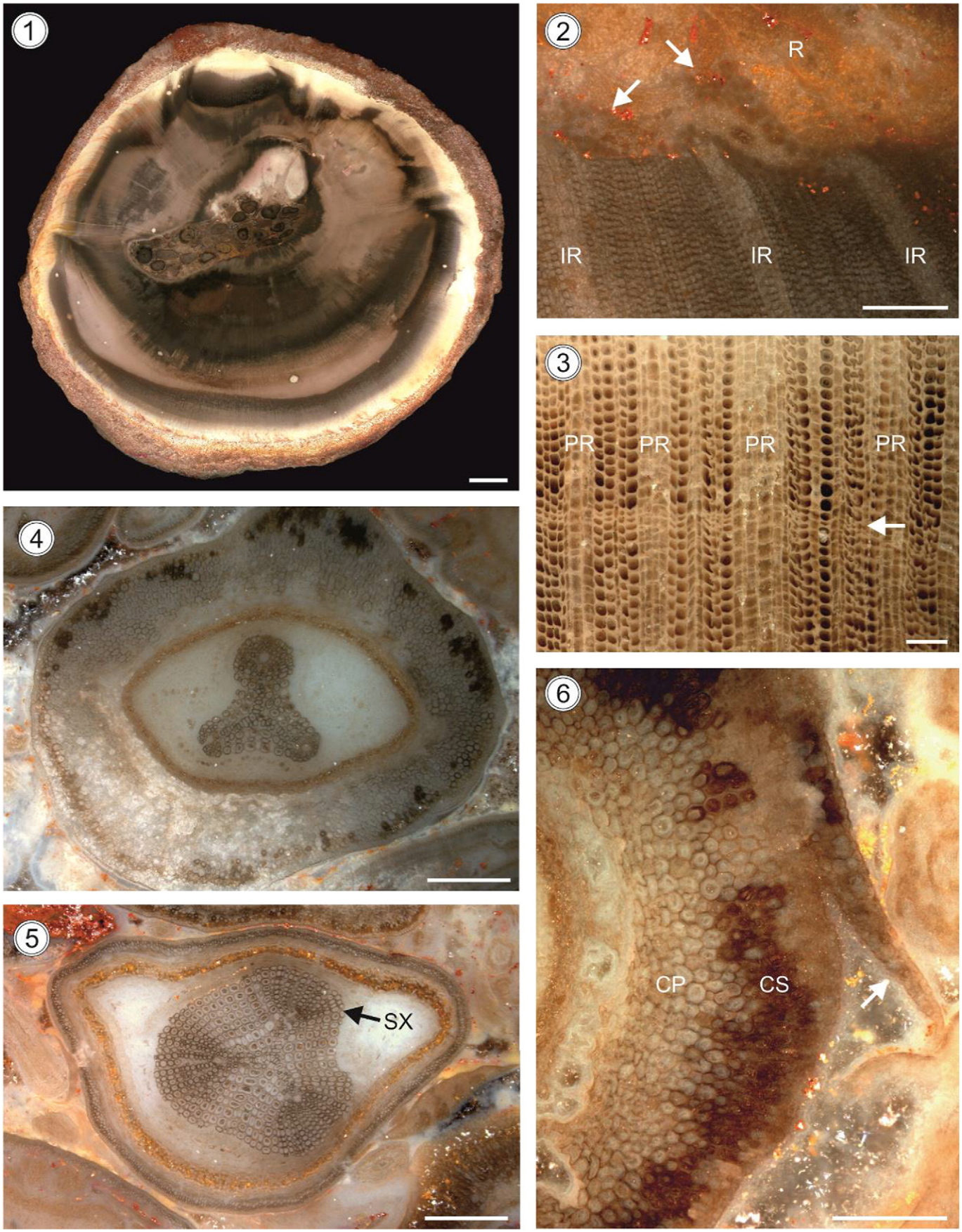

Plate IX (*caption on page 48*).

(Plate IX, 4–6). Detailed description of this fossil *Sphenophyllum* plant is beyond the scope of this study and will be given in a forthcoming paper. The wood of K 6040 is homogeneous without clear segmentation in fascicular wedges and interfascicular rays. A few growth ring-like density variations within the wood indicate seasonal or environmental changes (Plate IX, 3). Depending on the size of the specimen, the branch system may not be recognisable, but the sum of all other characters suggests specific assignment to *A. barthelii* sp. nov.

K 4874 is a stem portion 175 mm long and 106 mm in maximum diameter. The pith cavity measuring 4 × 5 mm is surrounded by 39 vascular segments. The secondary body has the same kind of homogeneous wood and shares anatomical characters with the aforementioned specimens.

4. Discussion

4.1. Comparisons of Arthropitys tocantinensis sp. nov. with previously described species

The studied specimens differ from *Arthropitys kansana* Andrews, 1952, *Arthropitys illinoensis* Anderson, 1954, *Arthropitys sterzelii* Rößler and Noll, 2010, and *Arthropitys cacundensis* Mussa and Coimbra, 1984 (in Coimbra and Mussa, 1984), in possessing exclusively scalariform pitting in the secondary xylem, whereas the other species have multiseriate circular pitting; *Arthropitys iannuzzii* Neregato et al., 2015 has multiseriate circular pitting and only few tracheids with scalariform pitting. Additionally, the branching system of the studied specimens is different from that of the aforementioned species.

Arthropitys bistriata (Cotta) Goeppert *emend*. Rößler et al., 2012, *Arthropitys communis* (Binney) Renault, 1896, *Arthropitys lineata* Renault, 1896, *Arthropitys versifoveata* Anderson, 1954, *Arthropitys deltoides* Cichan and Taylor, 1983, *Arthropitys junlianensis* Wang et al., 2003, *Arthropitys yunnanensis* (Tian and Gu) Wang et al., 2006, and *Arthropitys ezonata* Goeppert *emend*. Rößler and Noll, 2006 have, as the new species described here, scalariform pitting in their secondary xylem; *Arthropitys isoramis* Neregato et al., 2015 has both scalariform and multiseriate circular pitting, but all species cited above differ essentially in their branching system.

As a result, our new specimens are distinct from all *Arthopitys* species previously known and, therefore, they are classified as a new species, *Arthropitys tocantinensis* sp. nov. (see Tables 1 and 3, Fig. 2).

4.2. Comparisons of Arthropitys barthelii sp. nov. with previously described species

The studied specimens differ from *Arthropitys gigas* (Brongniart) Renault, 1896, *Arthropitys kansana* Andrews, 1952, *Arthropitys illinoensis* Anderson, 1954, *Arthropitys cacundensis* Mussa and Coimbra, 1984 (in Coimbra and Mussa, 1984), and *Arthropitys sterzelii* Rößler and Noll, 2010, with regard to their anatomy. The new material has exclusively scalariform thickening/pitting in their secondary xylem tracheids, whereas the other species bear multiseriate circular pitting; in *Arthropitys iannuzzii* Neregato et al., 2015, few tracheids has scalariform pitting but the majority of them shows multiseriate circular pitting. Moreover, the new material exhibits a different branching pattern in comparison to the species cited above.

The studied specimens are similar to *Arthropitys bistriata* (Cotta) Goeppert *emend*. Rößler et al., 2012, *Arthropitys communis* (Binney) Renault, 1896, *Arthropitys lineata* Renault, 1896, *Arthropitys versifoveata* Anderson, 1954, *Arthropitys deltoides* Cichan and Taylor, 1983, *Arthropitys junlianensis* Wang et al., 2003, *Arthropitys yunnanensis* (Tian and Gu) *ex* Wang et al., 2006, *Arthropitys ezonata* (Goeppert) *emend*. Rößler and Noll, 2006, regarding the scalariform pitting in the secondary xylem, however, the new specimens can be easily distinguished by their different branching patterns. *Arthropitys isoramis* Neregato et al., 2015, shows very regular branches, mostly 4 (rarely 3) per node, and presents both scalariform and multiseriate circular pitting on its tracheid's radial walls.

Considering these differences, the specimens studied here are distinct from all previously known species of *Arthropitys* and, therefore, classified as a new species, *Arthropitys barthelii* sp. nov. (see Tables 2 and 3, Fig. 3).

Table 1
Overview of the main anatomical and morphological data obtained from the holotype specimen of *Arthropitys tocantinensis* sp. nov.

Arthropitys tocantinensis sp. nov.				
Part of the plant Stem	Length 1850 mm	Diameter stem 130 × 213 mm at base 52 × 62 mm at top	Diameter pith 2 × 9 mm at base 9 × 20 mm at top	Girth 554 mm at base 180 mm at top
Morphology/branching	Branch system 3–12 branches at every node with and without secondary growth		Leaf traces 1.36 (1.11–1.61) mm height/0.43 (0.29–0.56) mm wide, in nodal position beneath branch traces	Root traces Departing at stem base with secondary growth
Internode length	63 mm, barely visible			
Primary tissues	Vascular strand number 55 at base 84 near top	Carinal canals (transverse section) radially/tangentially (μm) 290 (180–240)/210 (140–290), elliptical	Px tracheids/tyloses Not preserved	Mx tracheids (μm) 49 (13–120), circular to polygonal
Secondary tissues	Wood 25–89 mm, fascicular wedges and interfascicular rays only visible at pith periphery	Fascicular wedges width (μm), number files per fascicle (transverse section) Initially: 0.69 (0.45–0.88) mm, 27 files; Distally: only distinct initially	Tracheids (radial section) Scalariform thickenings Radially/tangentially (μm), (transverse section) Initially: 41 (30–70)/30 (22–50); Distally: 55 (40–70)/46 (20–70)	
	Interfascicular rays Width (μm), number files per fascicle (transverse section) Initially: 204 (100–340), 3–10 files; distally: indistinct	Cells (transverse section) Radially/tangentially (μm) Initially: 135 (50–210)/31 (18–70); Distally: indistinctly; cells pitted in the horizontal walls	Cells (radial section) Axially/radially (μm) 89 (50–170)/108 (73–140)	Cells (tangential section) Axially/tangentially (μm) 70 (30–170)/39 (10–70)
Cortex/periderm/special characters	not preserved			

Fig. 2. Proposed reconstruction of *Arthropitys tocantinensis* sp. nov. Drawing: Frederik Spindler (Freiberg, Germany).

4.3. Palaeoecological implications

Calamitaleans are unquestionably among the most common constituents of late Paleozoic plant communities, reported from various habitats and taphonomic settings including epiclastic and pyroclastic deposits (Renault, 1893, 1896; Gastaldo, 1992; Feng et al., 2012). In some cases, they even preserved in-situ (Dawson, 1851; Grand'Eury, 1877; DiMichele and Falcon-Lang, 2011). Although various organs, such as stems, leaves, reproductive organs and roots have been studied in great detail since the early days of paleobotany, several puzzling details of calamitalean growth and fossilisation remain. In pure clastic settings, the interpretation of their fossil remains as either pith casts (as traditionally thought) or stem casts, obviously remains equivocal (DiMichele and Falcon-Lang, 2012; Thomas, 2013; Falcon-Lang, 2015). Although true stem casts may be as common as pith casts and have long been studied especially from calamitaleans entombed in fine-grained pyroclastics (Petzholdt, 1841; Noll, 2000; Löcse et al., 2013; Rößler, pers. observations at ongoing Chemnitz excavations) it is challenging to address preservational circumstances and taphonomy for every site.

The siliceous petrified material from the Parnaíba Basin can contribute to this discussion in that these specimens preserved the exterior of the stems revealing morphological features on the whole-stem casts. Additionally, anatomically preserved large calamitaleans shed light on different aspects of growth and ecology. Recently, the root systems of some Permian calamitaleans were characterised including that of the here described *A. barthelii* sp. nov. (Rößler et al., 2014, p. 77 and text-fig. 4). An interpretation differing from the reed-like, fast-growing individuals reconstructed from the Pennsylvanian palaeoequatorial tropics was suggested (Rößler et al., 2014). Several new species recognised in the Permian of Brazil underline an unexpected diversity in growth form among these archaic arborescent sphenophytes (Neregato et al., 2015). Despite the striking conservatism in architecture and anatomy shared with their extant relatives (*Equisetum*), calamitaleans reveal a considerable adaptive range expressed in their branching and anatomy (Rößler et al., 2012). Not only their remarkable tolerance of disturbance or salinity (Gastaldo, 1992; Pfefferkorn et al., 2001) but also their outstanding architectural plasticity qualified them to survive severe environmental disturbances and climatic change up to the Lopingian (DiMichele et al., 2008). Here, the broadly defined *Arthropitys* incorporates species exhibiting characters, such as the common pitting of ray parenchyma, never documented before in this group but surprisingly present in every new species from Brazil. Recently, we re-investigated calamitaleans represented by free-stemmed woody trees that were anchored in the soil by numerous secondary roots (Neregato et al., 2015). Not only documented in Brazil, this quite unusual pattern among pteridophytes was confirmed by huge petrified calamitaleans from the type locality of Chemnitz in eastern Germany (Rößler et al., 2014) sharing with the Brazilian specimens site-specific features too. Although preserved in quite different ways, both depositional environments are characterised by clastic substrates and low-maturity soils without any peat accumulation (Luthardt et al., 2015). In contrast to the majority of much smaller individuals from nutrient-poor peat-forming mires (e.g., Josten, 1991; Cleal and Thomas, 1994; Galtier, 1997; Barthel, 2004; Opluštil et al., 2009), the largest calamitaleans known to date, *Arthropitys ezonata* from Chemnitz (Rößler and Noll, 2006), 60 cm in maximum diameter, and *Arthropitys* sp. (Rößler, 2014), 40 cm in maximum diameter, from Filadelfia, Tocantins, thrived as long-living individuals on mineral soils in seasonally influenced fluvial environments. In this respect we recognise obvious differences from the detailed ecological analysis and implications provided by Falcon-Lang (2015), but much accordance with the conclusions of DiMichele and Falcon-Lang (2012). Ultimately, further studies will be necessary to clarify the ecology of the group. Both sites, Tocantins and Chemnitz, also yielded noteworthy interactions among calamitaleans and their neighbouring plants. In Chemnitz, *Calamitea striata* was found surrounded by the climbing fern *Ankyropteris brongniartii* and its dense mats of adventitious aerial roots (Rößler and Noll, 2007). Whereas *Sphenophyllum* axes as isolated remains in fossiliferous cherts were documented a decade ago from the Parnaíba Basin (Dernbach et al., 2002), we can now present a peculiar interaction between a woody calamite stem, herein assigned to *Arthropitys barthelii* sp. nov., and at least 30 *Sphenophyllum* axes. The latter intruded into the calamite's pith cavity. Conspicuously narrow in this species, the pith cavity was considerably enlarged by cutting the internal wood segments (Plate IX, 2). Small coprolites abundant at this interface may indicate the cause of damage, namely arthropod xylophagy, as previously reported for other Brazilian calamitaleans showing pathogenic tissue reaction and abundant callus development (Rößler, 2006, Fig. 8b). Anatomical preservation of the *Sphenophyllum* axes (Plate IX, 4–6) show the steles to have variable amounts of secondary growth reflecting a range of ontogenetic stages, a multilayered parenchymatous to sclerenchymatous cortex, and the epidermal layer with attached leaves. Hence, this example preserved a particular “life snapshot” and reveals an additional ecological interaction between

Table 2
Overview of the main anatomical and morphological data obtained from the holotype specimen of *Arthropitys barthelii* sp. nov.

Arthropitys barthelii sp. nov.				
Part of the plant	Length	Diameter stem	Diameter pith	Girth
Stem	1280 mm	150 × 180 mm at base 104 × 114 mm at top	2.8 × 4.8 mm at base deformed at top	525 mm at base 342 mm at top
Morphology/branching	Branch system		Leaf traces	Adventitious roots
	2–17 branches per node, irregularly disposed, without secondary growth		Not preserved	Emerging vertically to slightly obliquely with secondary growth
Internode length	57 (40–80) mm, 21 measurements in total			
Primary tissues	Vascular strand number 25 at base 28 at 163 mm above lower end	Carinal canals radially/tangentially (μm) 160 (120–210)/140 (100–170)	Px tracheids/tyloses Not preserved	Mx tracheids diameter (μm) 34 (10–70), circular to polygonal
Secondary tissues	Wood 42–104 mm, relatively homogeneous with fascicular wedges and interfascicular rays only distinct in pith periphery	Fascicular wedges width (μm), number of files per fascicle (transverse section) Initially: 0.48 (0.32–0.74) mm, 1–3 tracheid files and 1–3 parenchyma files; distally: indistinct from IR	Tracheids (radial section) Scalariform thickenings and variable cross–field pitting Radially/tangentially (μm), (transverse section) initially: 45 (30–68)/37 (15–45); medially: 55 (47–69)/46 (35–60)	
	Interfascicular rays Width (μm), number files per fascicle (transverse section) Initially: 201 (100–420), 1–6 rectangular parenchyma; distally: cells indistinct from FR	Cells (transverse section) Radially/tangentially (μm) initially: 102 (55–220)/40 (20–85), pits in the horizontal cell walls distally: indistinctly pitted	Cells (radial section) Axially/radially (μm) 92 (50–220)/109 (65–220), brick–shaped with crossfield pits	Cells (tangential section) Diameter (μm) 84 (40–130)/43 (20–70) rectangular
Cortex/periderm/special characters	Not preserved			

perennial arboreal sphenophytes and their surrounding supposed ground cover or climbers.

5. Palaeophytogeographical implications

Several palaeogeographic reconstructions of the late Paleozoic outline the collision between Gondwana and Laurasia that resulted in the Pangaea landmass. Its amalgamation created a vast C-shaped landmass extending pole to pole with the central region close to the Equator and flanked to the east by the Tethys Ocean and to the west by the Panthalassa Ocean (Blakey, 2008; Fluteau et al., 2001; Scotese and Barret, 1990; Scotese and Langford, 1995; Ziegler et al., 1997). Owing to the global geological context, the end of the Carboniferous was marked by several changes shaping the supercontinent Pangaea (Parrish, 1995). Among these, the most relevant were: (1) The collision of Gondwana and Laurasia during the Permo-Pennsylvanian closed the equatorial epicontinental sea causing and generating active subduction along the coast being responsible for the formation of the Central Permian Mountains and for the disruption of the equatorial warm current (Ross and Ross, 1985; Tabor and Poulsen, 2008); (2) The sea level underwent changes with implications for oceanic circulation (Roscher and Schneider, 2006; Haq and Schutter, 2008); (3) The glaciation that spanned the Middle Pennsylvanian to Cisuralian was succeeded by a deglaciation process (Montañez and Poulsen, 2013). Thus, this set of factors in the late Pennsylvanian-Cisuralian was responsible for an extensive aridification of continental interiors. The climate was increasingly characterised by the transition from a cold humid climate to drier conditions, especially in Central and Western Pangaea, resulting in a

Table 3
Comparison among the type species *Arthropitys bistriata*, *Arthropitys tocantinensis* sp. nov., and *Arthropitys barthelii* sp. nov.

	Arthropitys bistriata	*Arthropitys tocantinensis* sp. nov.	*Arthropitys barthelii* sp. nov.
Fascicular wedges	Well defined throughout the wood	Well defined only in the innermost wood, more distally homogenous appearance of the wood in transverse section, but still delimited to interfascicular rays in tangential section	Well defined only in the innermost wood, more distally homogeneous appearance of the wood in both transverse and tangential sections
Thickening/pitting in secondary xylem (radial tracheid walls)	Scalariform pitting, very rare transitions to multiseriate circular pitting	Only scalariform pitting	Only scalariform pitting; broad-oval pitting in crossfield areas
Interfascicular rays (transverse section)			
Throughout secondary body	- Visible throughout the whole wood - No indication of pitted ray parenchyma	- Visible in innermost wood, indistinct in the external wood - Pitted ray parenchyma	- Visible only in the innermost wood, distally a homogeneous, parenchyma-rich wood appears - Pitted ray parenchyma
Tangential section			
% parenchyma cells	Up to 50%	35%	40%
Branching system			
Number of side branches (leafy twigs)	9–16 per whorl (whorl at every 5th to 9th node)	3–12 at every node but different size of neighbouring branch traces, in some cases overgrown during secondary growth	2–17 at every node, sometimes overgrown during secondary growth
Growth type of side branches (leafy twigs)	Without secondary growth	Without or with little secondary growth	Without secondary growth
Woody branches	At least 3 orders of woody branches	Woody branches present	Absent

Fig. 3. Proposed reconstruction of *Arthropitys barthelii* sp. nov. Drawing: Frederik Spindler (Freiberg, Germany).

striking floral and faunal provincialism (Dickins, 1993; Chumakov and Zharkov, 2002; Montañez and Poulsen, 2013; Parrish, 1995; Roscher and Schneider, 2006; Tabor and Poulsen, 2008).

In the Cisuralian, the Parnaíba Basin was positioned close to 30°S latitude, distant from tectonically active areas and marked climatically by a seasonal monsoonal regime (Faria and Truckenbrodt, 1980; Góes and Feijó, 1994; Pinto and Sad, 1986). This context is supported by several climate-sensitive indications. Faria and Truckenbrodt (1980) described evaporites, such as gypsum deposits in the Pedra de Fogo and Motuca formations; the fern *Buritiranopteris costata* (Tavares et al., 2014) clearly exhibits marked xeromorphic aspects in their fronds; frequent growth interruptions to secondary wood reflecting some kind of environmental seasonality were registered in several woody plants (Rößler, 2006; Kurzawe et al., 2013a,b; Rößler et al., 2014; Benício et al., 2015). Following Neregato et al. (2015) who described prominent tissue density variations in the secondary xylem of their new species *Arthropitys isoramis* and *A. iannuzzii* and interpreted them as growth rings, we report further evidence of growth-ring-like patterns in additional calamitalean taxa (*Arthropitys tocantinensis* sp. nov. and *A. barthelii* sp. nov.). Another striking indication of this climatic trend is exhibited in the petrified tissues of the new species. The silicification process requires alternation of humid and dry conditions to precipitate the silica into the cell lumina and intercellular spaces (Mussa and Coimbra, 1984; Jones et al., 1998; Matysová et al., 2010).

Besides this palaeoclimatic scenario, the Parnaíba Basin was positioned between two major floristic provinces, the Euramerican in the North and the Gondwanan in the South (Fig. 4). Generally speaking, the continental biotas especially plant communities underwent pronounced modifications over times according to climatic and geographical changes (DiMichele and Aronson, 1992). As pointed out by Mussa and Coimbra (1987), interactions between the Parnaíba Basin floristic associations and the classical Gondwana associations are to be expected. Additionally, it is worthwhile investigating influences of the Euramerican and/or Cathaysian floristic associations on the Parnaíba Basin flora.

Although detailed floristic studies in the Parnaíba Basin have been carried out only in recent years, 36 species within 25 genera (Table 4) have been identified. It is important to note that fossils preserved as adpressions, such as *Pecopteris* (Tavares, 2011), *Cyclostigma* and *Calamites* (Iannuzzi and Scherer, 2001), lycophytes found by the authors (unpublished data), and impressions of the callipterid foliage *Rhachiphyllum* aff. *schenkii* in association with fern pinnae of *Pecopteris* (Iannuzzi and Langer, 2014), all found in the Pedra de Fogo Formation, were not considered in our analyses because of their rarity or inadequate preservation.

From the petrified or permineralised genera (Table 5), the Parnaíba Basin shows the highest floristic similarity with Gondwana (42.8%), followed by Euramerica (33.3%) and Cathaysia (23.8%) (Fig. 4). Among the ferns, four genera are considered as endemic (*Tocantinorachis*, *Buritiranopteris*, *Dernbachia*, *Araguainorachis*), representing 50% of endemism within the group. In terms of non-endemic ferns, *Psaronius* and *Botryopteris* are cosmopolitan; *Tietea* is present in the Parnaíba Basin and in the Paraná Basin (Gondwana); and *Grammatopteris* in the Parnaíba Basin and Euramerica, although there are close relationships to *Rastropteris* found in the Cathaysian province (Galtier et al., 2001). Among the gymnosperms, *Carolinapitys*, *Cyclomedulloxylon*, *Teresinoxylon*, *Parnaiboxylon*, *Ductoabietoxylon* and *Scleroabietoxylon* are endemic, representing 54.5% of endemism within the group; *Amyelon* is cosmopolitan; *Cycadoxylon* is present in the Parnaíba Basin and Euramerica, and *Taeniopitys*, *Kaokoxylon*, and *Damudoxylon* in the Parnaíba Basin and Gondwana. In terms of sphenophytes, both *Arthropitys* and *Sphenophyllum* are cosmopolitan, whereas single anatomical characters, such as the pitted parenchyma in the Brazilian *Arthropitys* species seem to be unique in this genus.

It should be emphasized that the *Glossopteris*–type leaves seem to be totally absent from the Permian deposits of the Parnaíba Basin (Dolianiti, 1972; Mussa and Coimbra, 1987; Rohn and Rösler, 1987), whereas not so far southward, in Altiplano of Bolivia (Iannuzzi et al., 2004) and in the Paraná Basin (Rösler, 1978; Iannuzzi and Souza, 2005; Iannuzzi, 2010), this Gondwanan key genus is present. Consequently, a major and fairly sharp phytogeographic boundary and/or transition zone south of the Parnaíba Basin is suggested, limiting the

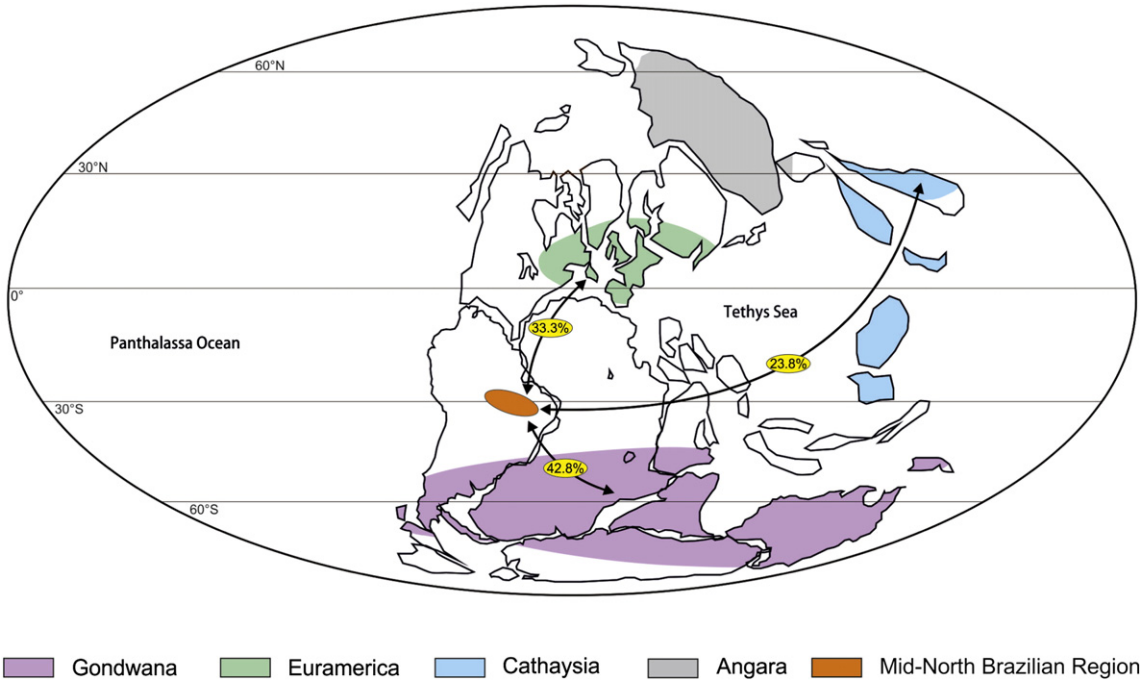

Fig. 4. The supercontinent Pangaea during the Cisuralian showing the proposed similarity among the floristic provinces. The values represent percentage similarities among Parnaíba Basin and the floristic provinces: Parnaíba Basin-Euramerica = 33.3%; Parnaíba Basin-Gondwana = 42.8%; Parnaíba Basin-Cathaysia = 23.8%. Floristic provinces according to Chaloner and Lacey (1973), Chaloner and Meyen (1973), Meyen (1987), and Cleal and Thomas (1991). Paleogeography after Scotese (1999).

distribution northwards of some typical Gondwanan elements in South America.

The most conspicuous consequence of the taxonomic findings of recent decades is the high level of endemism observed in the Parnaíba flora. Identified taxa include 11 shared genera (*Psaronius*, *Tietea*, *Grammatopteris*, *Botryopteris*, *Arthropitys*, *Sphenophyllum*, *Amyelon*, *Cycadoxylon*, *Taeniopitys*, *Kaokoxylon*, *Damudoxylon*), versus 10 endemic ones (*Tocantinorachis*, *Buritiranopteris*, *Dernbachia*, *Araguainorachis*, *Carolinapitys*, *Cyclomedulloxylon*, *Teresinoxylon*, *Parnaiboxylon*, *Scleroabietoxylon*, *Ductoabietoxylon*). Applying a simple formula commonly used in modern biogeography to determine the level of endemism of a region (Cox and Moore, 2005), i.e., [number of endemic taxa × 100 / total number of taxa], results in an estimate of 47.6% endemic genera for this flora (Fig. 4). This value suggests that the Parnaíba Basin flora belongs to a distinct phytogeographic unit, which could perhaps be ranked as a new Floral Region according to criteria proposed by Wnuk (1996) for the late Paleozoic.

Cluster analysis remains one of the most useful methods for biogeographical approaches (Kovach, 1988; Hammer et al., 2001). The Jaccard Coefficient is also a very powerful tool for analysing data regarding presence-absence with no importance on abundance (Legendre and Legendre, 1998; Hammer et al., 2001). Thus, cluster and Jaccard Coefficient analyses were undertaken to compare some Moscovian to Cisuralian anatomically preserved floras presented by Hilton and Cleal (2007), augmented by European floras from the Perdasdefogu Basin, Sardinia/Italy (Galtier et al., 2011), Grand-Croix, Saint-Étienne Basin, and Autun/France (Galtier, 2008), Leukersdorf Formation of the Petrified Forest of Chemnitz/Germany (Rößler, 2006), Semily and Vrchlabí formations from Krkonoše Piedmont Basin/Nova Paka/Czech Republic (data provided by Dr. Vaclav Mencl, 2015), and Irati Formation from the Paraná Basin, southern Brazil (Mussa, 1978a,b, 1982, 1986; Mussa et al., 1980; Merlotti, 2009; Merlotti and Kurzawe, 2011). Hilton and Cleal (2007) presented an analysis of 19 Euramerican and Cathaysian floras, ranging from early Bashkirian up to Asselian-Sakmarian age. Considering that the Motuca Formation is probably Cisuralian (Cisneros et al., 2015; Conceição et al., 2016a), the current analysis includes only the Moscovian and Asselian-Sakmarian floras.

The analysis has shown that the Parnaíba Basin does not have strong similarity with any other flora analysed herein (Fig. 5 and Table 6). This result reflects the fact that despite the Parnaíba flora sharing a considerable number of taxa with typical floras from the tropics and those of Gondwanan floristic province (Fig. 4; Table 5), it also reveals a high degree of endemism, both at specific and generic levels. Even when the Parnaíba Basin flora is compared to that of the Irati Formation of the Paraná Basin, the region hosting the closest fossil floras little similarity has been found.

In fact, the position of the Parnaíba Basin flora in middle latitudes, i.e., halfway between the temperate to cold regions of Gondwana and the equatorial floristic belt, well explains the results obtained from the cluster analysis. Despite all the palaeogeographic reconstructions for the Permian including the region of the Parnaíba Basin within a belt of warm climates (Rees et al., 1999, 2002; Boucot et al., 2013), none of them attributed the existence of favourable conditions for the development of tropical forests. Whether using data from climate-sensitive sediments (Boucot et al., 2013), or by using data derived from climate and vegetation model simulations (Rees et al., 1999, 2002), the region occupied by the Parnaíba Basin has always been considered as having hosted desert regimes, with arid-to-semiarid climates, during the Permian. These interpretations do not match with the extensive record of a diverse flora incorporating hygrophilous arborescent (>10 m high) of pteridophytes and gymnosperms (Capretz and Rohn, 2013) evident in this basin. Silica-petrified forests have been found in Permian deposits [e.g., Pedra de Fogo and Motuca formations] that are widely distributed from the southwest to northeast rims of the Parnaíba Basin, covering >800 km of a narrowly outcropping fossiliferous belt. It is hard to imagine that there was no climatic variation over this vast floristic region (Rößler and Noll, 2002a,b; Capretz and Rohn, 2013; Conceição et al., 2016b).

There are several indicators in the Parnaíba floral record pointing to a seasonally dry climate regime, such as: a) the climatic-driven process of silicification (Matysová et al., 2010); b) the braided fluvial system generating the depositional settings (Capretz and Rohn, 2013); c) the occurrence of evaporites and gypsum deposits (Faria and Truckenbrodt, 1980); d) the noticeable xeromorphic features found in the fern fronds

Table 4
Plant fossils found in the Parnaíba Basin.

Taxon	Localities	References	Age	Some occurrences of the genera
Psaronius brasiliensis	Oieras/São Gonçalo do Amarante (PI), Araguaína/Filadélfia (TO)	Brongniart (1872), Rößler & Noll (2002)	–	Brazil (Paraná Basin), Germany, France, USA, China
Psaronius arrojadoi	Chapada do Jaboti (MA), TFTNM	Pelourde (1914), Herbst (1985), Tavares (2011)	Early Permian (Herbst, 1985)	Brazil (Paraná Basin), Germany, France, USA, China
Psaronius sinuosus	Araguaína (TO)	Herbst (1999), Rößler & Noll (2002)	Early Permian (Herbst, 1999)	Brazil (Paraná Basin), Germany, France, USA, China
Tietea singularis	Araguaína (TO), TFTNM	Herbst (1986), Rößler & Noll (2002), Tavares (2011)	Permian (Herbst, 1986)	Brazil (Paraná Basin)
Tietea derbyi	Carolina (MA)	Herbst (1992)	Permian	Brazil (Paraná Basin)
Tocantinorachis buritiranaensis	TFTNM	Tavares (2011)	Early Permian	Endemic
Pecopteris sp.	TFTNM	Tavares (2011)	Early–Middle Permian	Cosmopolitan
Buritiranopteris costata	TFTNM	Tavares et al. (2014)	Early Permian	Endemic
Grammatopteris freitasii	Araguaína/Filadélfia (TO)	Rößler & Galtier (2002a)	Permian (Rößler & Galtier, 2002a)	Germany, France
Dernbachia brasiliensis	Araguaína/Filadélfia (TO)	Rößler & Galtier (2002b)	Permian (Rößler & Galtier, 2002b)	Endemic
Botryopteris nollii	Araguaína/Filadélfia (TO)	Rößler & Galtier (2003)	Permian (Rößler & Galtier, 2003)	Germany, France, Belgium, USA, China
Araguainorachis simplissima	Carolina (MA)/Riachão (TO)	Mussa & Coimbra (1987)	Early–Middle Permian	Endemic
Cyclostigma brasiliensis	Carolina (MA)	Iannuzzi & Scherer (2001)	Early Permian	UK, China, Japan
Arthropitys cacundensis	Araguaína (TO), Carolina (MA)	Coimbra & Mussa (1984)	Middle Carboniferous–Early Permian	Germany, France, England, USA, China, Czech Republic
Arthropitys isoramis	TFTNM	Neregato et al. (2015)	Early Permian	Germany, France, England, USA, China, Czech Republic
Arthropitys iannuzzii	TFTNM	Neregato et al. (2015)	Early Permian	Germany, France, England, USA, China, Czech Republic
Arthropitys tocantinensis	TFTNM	This work	Early Permian	Germany, France, England, USA, China, Czech Republic
Arthropitys barthelii	TFTNM	This work	Early Permian	Germany, France, England, USA, China, Czech Republic
Calamites sp.	Carolina (MA)	Iannuzzi & Scherer (2001)	Early Permian	England, Holland, Germany, France, Belgium, USA, China, Brazil (Paraná Basin)
Sphenophyllum sp.	Araguaína/Filadélfia (TO)	Rößler & Noll (2002)	Permian	Cosmopolitan
Amyelon bieloi	Between Araguaína (TO) and Carolina (MA)	Coimbra & Mussa (1984)	Middle Carboniferous–Early Permian	England, USA, Scotland, China, France
Carolinapitys maranhensis	Between Araguaína (TO) and Carolina (MA)	Coimbra & Mussa (1984)	Middle Carboniferous–Early Permian	Endemic
Cyclomedulloxylon parnaibense	Carolina (MA)/Riachão (TO)	Mussa & Coimbra (1987)	Early–Middle Permian	Endemic
Cycadoxylon brasiliense	Carolina/Riachão (TO)	Mussa & Coimbra (1987)	Early–Middle Permian	France, England

Table 4 (*continued*)

Teresinoxylon euzebioi	Teresina (PI)	Caldas et al. (1989)	Early–Middle Permian	Endemic
Parnaiboxylon sp.	TFTNM	Kurzawe et al. (2013a)	Permian	Endemic
Parnaiboxylon rohnae	TFTNM	Kurzawe et al. (2013a)	Permian	Endemic
Scleroabietoxylon chordas	TFTNM	Kurzawe et al. (2013a)	Permian	Endemic
Ductoabietoxylon solis	TFTNM	Kurzawe et al. (2013a)	Permian	Endemic
Taeniopitys tocantinensis	TFTNM	Kurzawe et al. (2013b)	Permian	Antarctica
Taeniopitys sp.	TFTNM	Kurzawe et al. (2013b)	Permian	Antarctica
Kaokoxylon punctatum	TFTNM	Kurzawe et al. (2013b)	Permian	India, Australia, South Africa, Argentina, Antarctica
Damudoxylon buritiranaensis	TFTNM	Kurzawe et al. (2013b)	Permian	India, Australia, South Africa
Damudoxylon humile	TFTNM	Kurzawe et al. (2013b)	Permian	India, Australia, South Africa
Damudoxylon roesslerii	TFTNM	Kurzawe et al. (2013b)	Permian	India, Australia, South Africa
Rhachiphyllum schenkii	Nova Iorque (MA)	Iannuzzi & Langer (2013)	Late Carboniferous–Early Permian	USA, north Africa, Germany, France, Russia, China, Malay, southeast Asia

TO = Tocantins State, MA = Maranhão State, PI = Piauí State, TFTNM = Tocantins Fossil Trees Natural Monument. In the left column, green representing ferns, yellow lycophytes, pink sphenophytes, and blue gymnosperms.

of *Buritiranopteris costata* (Tavares et al., 2014); e) the growth-ring-like patterns found in *Arthropitys* stems (Neregato et al., 2015), roots (Rößler et al., 2014), and in associated gymnosperms (Kurzawe et al., 2013a, 2013b; Benício et al., 2015). However, availability of water must have existed annually to support the diversity of plant groups and their arborescent stature. The majority of trees may have grown over several years to reach such dimensions, both in diameter and in height. Based on all these considerations, the modern biome that best equates with the floral register from the Parnaíba Basin is that of "Tropical summerwet" following the climate modelling established by Rees et al. (2002).

Therefore, instead of being understood as a transitional floristic belt, the Parnaíba Basin should be considered a unique region occupied by a flora constituting its own phytogeographic unit. The palaeogeographic (approx. 30° south), climatic (tropical warm semiarid) and sedimentary (braided fluvial system) data support this conclusion, indicating a set of biotic and abiotic features exclusive to this region, which explains the development of a diverse flora adapted to these unique conditions. Therefore, we propose formally a new phytogeographic unit named herein as the "Mid-North Brazilian Region" based on the Parnaíba flora, representing the record of tropical summerwet climate that existed in the southern mid-latitudes of northern Gondwana during the Cisuralian (Fig. 5). Unfortunately, any equivalent early Permian anatomically preserved floras are known in north-western South America or in central-north Africa that could be attributed to this province until now. Nonetheless, this new unit fits quite well with previous records describing the occurrence of so-called "Tropical Gondwana", a belt having Euroamerican adpressed floras that was distributed by the north rim of West Gondwana, including the northwestern of South America (e.g., Venezuela; Ricardi-Branco, 2008) and northern Africa (Chaloner and Meyen, 1973; Lejal-Nicol, 1985; Doubinger and Roy-Dias, 1985).

Table 5
Petrified or permineralised genera occurring in the Parnaíba Basin and in Gondwana, Euramerica, and Cathaysia.

	Parnaíba Basin	Euramerica	Gondwana	Cathaysia
Psaronius	x	x	x	x
Tietea	x	–	x	–
Tocantinorachis	x	–	–	–
Buritiranopteris	x	–	–	–
Grammatopteris	x	x	–	–
Dernbachia	x	–	–	–
Botryopteris	x	x	x	x
Araguainorachis	x	–	–	–
Arthropitys	x	x	x	x
Sphenophyllum	x	x	x	x
Amyelon	x	x	x	x
Carolinapitys	x	–	–	–
Cyclomedulloxylon	x	–	–	–
Cycadoxylon	x	x	–	–
Teresinoxylon	x	–	–	–
Parnaiboxylon	x	–	–	–
Scleroabietoxylon	x	–	–	–
Ductoabietoxylon	x	–	–	–
Taeniopitys	x	–	x	–
Kaokoxylon	x	–	x	–
Damudoxylon	x	–	x	–

References in the Parnaíba Basin: *Psaronius*: Pelourde (1914), Brongniart (1872), Herbst (1985, 1999), Röβler and Noll (2002), Tavares (2011); *Tietea*: Herbst (1986, 1992), Rößler and Noll (2002), Tavares (2011); *Pecopteris*: Tavares (2011); *Grammatopteris*: Rößler and Galtier (2002a); *Botryopteris*: Rößler and Galtier (2003); *Arthropitys*: Coimbra and Mussa (1984), Rößler and Noll (2002), Neregato et al. (2015); *Sphenophyllum*: Rößler and Noll (2002); *Amyelon*: Coimbra and Mussa (1984); *Cycadoxylon*: Mussa and Coimbra (1987); *Taeniopitys*: Kurzawe et al. (2013b); *Kaokoxylon*: Kurzawe et al. (2013b); *Damudoxylon*: Kurzawe et al. (2013b); In the left column, green representing ferns, pink sphenophytes, and blue gymnosperms.

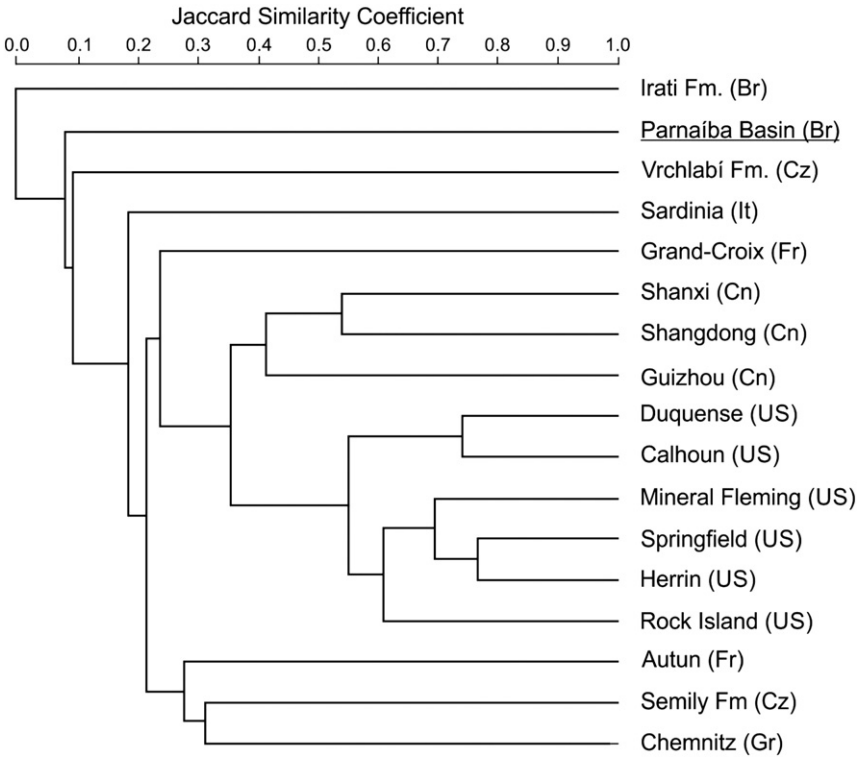

Fig. 5. Cluster analysis among late Carboniferous - Cisuralian floras and those of the Parnaíba Basin. The data used in this analysis are shown in the Supplementary data.

Lastly, it is worth mentioning that perhaps the discrepancy observed by the presence of this flora in the Mid-North Brazilian Region with that expected from the climate model represents an aberration caused by the occurrence of large inland water bodies widely distributed and interconnected in the northeast of the South American continent, which might have provided higher moisture levels on the lowlands of this region. Unfortunately, the effects of the presence of epeiric seas on regional climates have not been adequately accounted for in the palaeogeographic reconstructions or climate modelling, but their consequences should be considered.

6. Conclusions

1) Present investigations reveal much more anatomical and growth form diversity among low-latitude Permian calamitaleans of Gondwana. Although of overall similarity and easily recognisable at generic level, there are several anatomical or branching characteristics enabling segregation of these arborescent pteridophytes at species level.
2) Based on their anatomical and branching characteristics two new species, *Arthropitys tocantinensis* sp. nov. and *Arthropitys barthelii* sp. nov., are introduced. Both species share the peculiar pitting of parenchyma with the recently described species *Arthropitys isoramis* and *Arthropitys iannuzzii*.
3) Although sharing similar systems of stem or branch construction and secondary adventitious roots, these Permian calamitaleans have considerable plasticity in the morphological and anatomical development of all plant organs.
4) Stems, branches and roots are parenchyma-rich organs, which can show considerable secondary growth. Like an archive of environmental fluctuations the resulting wood regularly exhibits growth-ring-like tissue density variations reflecting seasonal changes in the palaeoenvironment.

Table 6
Jaccard Coefficient among Parnaíba Basin flora with some Moscovian to Cisuralian floras around the world.

Locality	Age (Ma)	Jaccard coefficient among Late Carboniferous – Cisuralian floras and Parnaíba Basin
Vrchlabí Fm (Cz)	298.9–295.0 (Martínek and Štolfova, 2009)	0.041667
Irati Fm (Br)	278.4 ± 2.2 (Santos et al., 2006)	0.046512
Springfield (US)	315.2–307.0 (Hilton and Cleal, 2007)	0.055556
Herrin (US)	315.2–307.0 (Hilton and Cleal, 2007)	0.056604
Grand-Croix (Fr)	307.0–298.9 (Galtier, 2008)	0.060241
Mineral-Flemming (US)	315.2–307.0 (Hilton and Cleal, 2007)	0.075472
Calhoun (US)	307.0–298.9 (Hilton and Cleal, 2007)	0.078431
Shangdong (Cn)	298.9–290.1 (Hilton and Cleal, 2007)	0.083333
Shanxi (Cn)	298.9–290.1 (Hilton and Cleal, 2007)	0.085106
Rock Island (US)	315.2–307.0 (Hilton and Cleal, 2007)	0.086957
Duquense (US)	307.0–298.9 (Hilton and Cleal, 2007)	0.086957
Semily Fm. (Cz)	303–7–301(Martínek and Štolfova, 2009)	0.096774
Sardinia (It)	298.9–290.1 (Galtier et al., 2011)	0.1
Autumn (Fr)	298.9–272.3 (Galtier, 2008)	0.102041
Chemnitz (Gr)	290.6 ± 1.8 (Rößler et al., 2012)	0.108108
Guizhou (Cn)	–	0.125

Data used in this analysis are shown in the Supplementary data.

5) We report the striking intergrowth of *Arthropitys barthelii* sp. nov. with *Sphenophyllum*, up to 30 axes of the latter showing different ontogenetic stages and growing inside the calamite's pith that was previously excavated by arthropod boring.
6) Based on a set of biotic and abiotic features exclusive to the Parnaíba Basin, a new palaeophytogeographic province is formally proposed herein as the "Mid-North Brazilian Region" representing a diverse flora adapted to a tropical summerwet climate that existed in the southern low- to mid-latitudes of northern Gondwana during the Cisuralian.

Acknowledgements

We would like to thank the Brazilian Research Council ("Conselho Nacional de Desenvolvimento Científico e Tecnológico" – CNPq) for the PhD scholarship (Process 141365/2008-0) to the first author (RN), for financial support to the project in the Parnaíba Basin (Process 483704/2010-5), and grants (PQ 305687/2010-7 and PQ 309211/2013-1) to Roberto Iannuzzi. Acknowledgements are also due to the Deutsche Forschungsgemeinschaft (DFG grant RO 1273/3-1 to R.R.). We are indebted to Dr. Václav Mencl, Nová Paka, for providing palaeofloristic data from the Krkonoše Piedmont Basin. Dr. Jason Hilton (University of Birmingham) and Dr. Christopher Cleal (National Museum Wales, Cardiff) kindly provide the data used in the cluster analysis. Dr. Jean Galtier (Montpelier) is acknowledged for valuable comments concerning anatomical features and Ludwig Luthardt (Chemnitz) kindly shared his knowledge on climate-induced wood growth. Finally, this manuscript greatly benefited from the detailed helpful suggestions provided by two anonymous reviewers and the editor, Hans Kerp.

Appendix A. Supplementary data

Supplementary data to this article can be found online at http://dx.doi.org/10.1016/j.revpalbo.2016.11.001.

References

Anderson, B.R., 1954. A study of American petrified calamites. Ann. Mo. Bot. Gard. 41, 395–418.
Andrews, H.N., 1952. Some American petrified calamitean stems. Ann. Mo. Bot. Gard. 39, 189–206.
Barthel, M., 2004. Die Rotliegendflora des Thüringer Waldes. Teil 2: Calamiten und Lepidophyten. Veröffentlichungen des Naturhistorischen Museums Schleusingen 19, 19–48.
Benício, J.R.W., Spiekermann, R., Manfroi, J., Uhl, D., Pires, E.F., Jasper, A., 2015. Paleoclimatic inferences based on dendrological patterns of permineralized wood from the Permian of the northern Tocantins Petrified Forest, Parnaíba Basin, Brazil. Paleobio. Paleoenv http://dx.doi.org/10.1007/s12549-015-0218-8.
Blakey, R.C., 2008. Gondwana paleogeography from assembly to breakup – a 500 m.y. odyssey. Geol. Soc. Am. Spec. Pap. 441, 1–28.
Boucot, A.J., Xu, C., Scotese, C.R., Morley, R.J., 2013. Phanerozoic Paleoclimate: an atlas of lithologic indicators of climate. SEPM Concepts in Sedimentology and Paleontology 11. Folio, p. 478.
Brongniart, A., 1872. Notice sur le Psaronius brasiliensis. Bull. Soc. Bot. France, Ser. 5 (19), 3–10.
Capretz, R.L., Rohn, R., 2013. Lower Permian stems as fluvial paleocurrent indicators of the Parnaíba Basin, northern Brazil. J. S. Am. Earth Sci. 45, 69–82.
Chaloner, W.G., Lacey, W.S., 1973. The distribution of Late Paleozoic Flora. In: Hughes, N.F. (Ed.), Organisms and Continents Through Time. Methods for Assessing Relationships Between Past and Present Biologic Distribution and the Position of ContinentsSpec. Pap. Palaeontol 12. Palaeontological Association, London, pp. 271–289.
Chaloner, W.G., Meyen, S.V., 1973. Carboniferous and permian floras of the northern continents. In: Hallan, A. (Ed.), Atlas of Paleobiogeography. Elsevier, Amsterdam, pp. 169–186.
Chumakov, N.M., Zharkov, M.A., 2002. Climate during Permian-Triassic biosphere reorganizations, article 1: climate of the early Permian. Stratigr. Geol. Correl. 10, 586–602.
Cichan, M.A., Taylor, T.N., 1983. A systematic and developmental analysis of *Arthropitys deltoides* sp. nov. Bot. Gaz. 144, 285–294.
Cisneros, J.C., Marsicano, C., Angielczyk, K.D., Smith, R.M.H., Richter, M., Fröbisch, J., Kammerer, C.F., Sadleir, R.W., 2015. New Permian fauna from tropical Gondwana. Nat. Commun. 6, 8676.
Cleal, C.J., Thomas, B.A., 1991. Carboniferous and Permian palaeogeography. In: Cleal, C.J. (Ed.), Plant Fossils in Geological Investigation: The Paleozoic. Ellis Horwood Ltd., England, pp. 155–181.
Cleal, C.J., Thomas, B.A., 1994. Plant Fossils of the British Coal Measures. Palaeontological Association, London (222 pp).
Coimbra, A.M., Mussa, D., 1984. Associação lignitafoflorística na Formação Pedra-de-Fogo, (Arenito Cacunda), Bacia do Maranhão - Piauí, Brasil. XXXIII Congresso Brasileiro de Geologia. Sociedade Brasileira de Geologia, Rio do Janeiro, pp. 591–605.
Conceição, D.M., Andrade, L.S., Cisneros, J.C., Iannuzzi, R., Pereira, A.A., Machado, F.C., 2016a. New petrified forest in Maranhão, Permian (Cisuralian) of the Parnaíba Basin, Brazil. J. S. Am. Earth Sci. 70, 308–323.
Conceição, D.M., Cisneros, J.C., Iannuzzi, R., 2016b. Novo registro de uma Floresta Petrificada em Altos, Piauí: relevância e estratégias para geoconservação. Pesquisas em Geociências 43, 311–324.
Cox, C.B., Moore, P.D., 2005. Biogeography: An Ecological and Evolutionary Approach. seventh ed. Blackwell Publishing, Oxford (440 pp).
Dawson, J.W., 1851. Notice on the occurrence of upright *Calamites* near Pictou, Nova Scotia. Quarterly J. Geological Soc. London 7, 194–196.
Dernbach, U., Roll, R., Rößler, R., 2002. News from Araguaina, Brazil. In: Dernbach, U., Tidwell, W.D.I. (Eds.), Secrets of Petrified Plants - Fascination From Millions of Years. D'Oro-Verlag, Heppenheim, pp. 78–87.
Dias-Brito, D., Rohn, R., Castro, J.C., Dias, R.R., Rössler, R., 2007. Floresta Petrificada do Tocantins Setentrional – O mais exuberante e importante registro florístico tropical-subtropical permiano no Hemisfério Sul. In: Winge, M., Schobbenhaus, C., Berbert-Born, M., Queiroz, E.T., Campos, D.A., Souza, C.R.G., Fernandes, A.C.S. (Eds.), Sítios Geológicos e Paleontológicos do Brasil. DNPM/CPRM-SIGEP, Brasília. Available online 23/01/2007 at: http://www.unb.br/ig/sigep/sitio104/sitio104english.pdf, (14 pp).
Dickins, J.M., 1993. Climate of the Late Devonian to Triassic. Palaeogeogr. Palaeoclimatol. Palaeoecol. 100, 89–94.
DiMichele, W.A., Aronson, R.B., 1992. The Pennsylvanian-Permian vegetation transition: a terrestrial analogue to the onshore-offshore hypothesis. Evolution 46, 807–824.
DiMichele, W.A., Falcon-Lang, H.J., 2011. Fossil forests in growth position (T^0 assemblages): origin, taphonomic biases and palaeoecological significance. J. Geol. Soc. 168, 585–605.
DiMichele, W.A., Falcon-Lang, H.J., 2012. Calamitalean pith casts reconsidered. Rev. Palaeobot. Palynol. 173, 1–14.
DiMichele, W.A., Kerp, H., Tabor, N.J., Looy, C.V., 2008. The so-called "Paleophytic–Mesophytic" transition in equatorial Pangea – multiple biomes and vegetational tracking of climate change through geological time. Palaeogeogr. Palaeoclimatol. Palaeoecol. 268, 152–163.
Dolianiti, E., 1972. Relações entre as floras paleozóicas do Brasil. An. Acad. Bras. Cienc. 44, 113–118.
Doubinger, J., Roy-Dias, C., 1985. La paléoflore du Stéphanien de l'Oued Zat (Haut-Atlas de Marrakech, versant nord, Marroc). Geobios 18, 575–594.
Falcon-Lang, H.J., 2015. A calamitalean forest preserved in growth position in the Pennsylvanian coal measures of South Wales: implications for paleoecology, ontogeny and taphonomy. Rev. Palaeobot. Palynol. 214, 51–67.
Faria Jr., L.E.C., Truckenbrodt, W., 1980. Estratigrafia e petrografia da Formação Pedra de Fogo – Permiano da Bacia do Parnaíba. XXXI Congresso Brasileiro de Geologia 2. Sociedade Brasileira de Geologia, Camboriú, pp. 740–754.
Feng, Z., Zierold, T., Rößler, R., 2012. When horsetails became giants. Chin. Sci. Bull. 57, 2285–2288.
Fluteau, F., Besse, J., Broutin, J., Ramstein, G., 2001. The Late Permian climate. What can be inferred from climate modeling concerning Pangaea scenarios and Hercynian range altitude? Palaeogeogr. Palaeoclimatol. Palaeoecol. 167, 39–71.
Galtier, J., 1997. Coal-ball floras of the Namurian-Westphalian of Europe. Rev. Palaeobot. Palynol. 95, 51–72.
Galtier, J., 2008. A new look at the permineralized flora of Grand-Croix (Late Pennsylvanian, Saint-Etienne basin, France). Rev. Palaeobot. Palynol. 152, 129–140.
Galtier, J., Wang, S.J., Li, C.S., Hilton, J., 2001. A new genus of filicalean fern from the Lower Permian of China. Bot. J. Linn. Soc. London 147, 429–442.
Galtier, J., Ronchi, A., Broutin, J., 2011. Early Permian silicified floras from the Perdasdefogu Basin (SE Sardinia): comparison and bio-chronostratigraphic correlation with the floras of the Autun Basin (Massif Central, France). Geodiversitas 33, 43–69.
Gastaldo, R.A., 1992. Regenerative growth in fossil horsetails (*Calamites*) following burial by alluvium. Hist. Biol. 6, 203–220.
Goeppert, H.R., 1864–1865. Die fossile Flora der Permischen formation. Palaeontographica 12, 1–124.
Góes, A.M.O., Feijó, F.J., 1994. Bacia do Parnaíba. Boletim de Geociências da Petrobrás 8, 57–67.
Grand'Eury, C.F., 1877. Mémoire sur la flore Carbonifère du département de La Loire et du centre de la France. Mém. Acad. Sci. Inst. Nat. Fr. 24 (624 pp).
Hammer, Ø., Harper, D.A.T., Ryan, P.D. 2001. PAST: Paleontological statistics software package for education and data analysis. Available at: http://paleo-electronica.org/2001_1/past/issue1_01.htm.
Haq, B.U., Schutter, S.R., 2008. A chronology of Paleozoic sea-level changes. Science 322, 64–68.
Herbst, R., 1985. Nueva descripcion de *Psaronius arrojadoi* (Pelourde) (Marattiales), del Permico de Brasil. Ameghiniana 21, 243–258.
Herbst, R., 1986. Studies on Psaroniaceae. I. The family Psaroniaceae (Marattiales) and a Redescription of *Tietea singularis* Solms-Laubach, From the Permian of Brazil. IV Congresso Argentino de Paleontologia y Bioestratigrafia. Asociación Paleontológica Argentina, Mendoza, pp. 163–171.
Herbst, R., 1992. Studies on Psaroniaceae. III. *Tietea derbyi* n. sp., from the Permian of Brazil. Cour. Forschungsinst. Senckenb. 147, 155–161.
Herbst, R., 1999. Studies on Psaroniaceae. IV. Two species of *Psaronius* from Araguaína, state of Tocantins, Brazil. Facena 15, 9–18.
Hilton, J., Cleal, C.J., 2007. The relationship between Euramerican and Cathaysian tropical floras in the Late Palaeozoic: Palaeobiogeographical and palaeogeographical implications. Earth-Sci. Rev. 85, 85–116.

Iannuzzi, R., 2010. The flora of early Permian coal measures from the Paraná Basin in Brazil: a review. Int. J. Coal Geol. 83, 229–247.
Iannuzzi, R., Langer, M.C., 2014. The presence of callipterids in the Permian of northeastern Brazil: stratigraphic and phytogeographical implications. In: Rocha, R., Pais, J., Kullberg, J.C., Finney, S. (Eds.), STRATI 2013: First International Congress on Stratigraphy. Springer Geology, Cham, pp. 403–406.
Iannuzzi, R., Scherer, C.M.S., 2001. Vegetais fósseis carbonificados na Formação Pedra-de-Fogo, Bacia do Paranaíba, TO-MA: significado paleoambiental. II Simpósio sobre a Bacia do Araripe e bacias interiores do Nordeste, Crato, 1997. Sociedade Brasileira de Paleontologia, Fortaleza, pp. 129–139.
Iannuzzi, R., Souza, P.A., 2005. Floral succession in the Lower Permian deposits of the Brazilian Paraná Basin: an up-to-date overview. Bull. New Mexico Museum Natural History and Science 30, 144–149.
Iannuzzi, R., Vieira, C.E.L., Sommer, M.G., Díaz-Martínez, E., Grader, G.W., 2004. Permian plants from the Chutani formation (Titicaca Group, northern Altiplano of Bolivia): II. The morphogenus *Glossopteris*. An. Acad. Bras. Cienc. 76, 129–138.
Jones, B., Renaut, R.W., Rosen, M.R., Klyen, L., 1998. Primary siliceous rhizoliths from loop road Hot Springs, North Island, New Zealand. J. Sediment. Res. 68, 115–123.
Josten, K.-H., 1991. Die Steinkohlen-Floren Nordwestdeutschlands. Fortschritte Geologie Rheinland und Westfalen. 36 (434 pp).
Kovach, W.L., 1988. Multivariate methods of analyzing paleoecological data. In: DiMichele, W.A., Wing, S.L. (Eds.), Methods and Applications of Plant Paleoecology. The Paleontological Society Spec. Publ. 3, pp. 72–104 (Tennessee).
Kurzawe, F., Iannuzzi, R., Merlotti, S., Rößler, R., Noll, R., 2013a. New gymnospermous woods from the Permian of the Parnaíba Basin, northeastern Brazil, part I: *Ductoabietoxylon*, *Scleroabietoxylon* and *Parnaiboxylon*. Rev. Palaeobot. Palynol. 195, 37–49.
Kurzawe, F., Iannuzzi, R., Merlotti, S., Rohn, R., 2013b. New gymnospermous woods from the Permian of the Parnaíba Basin, northeastern Brazil, part II: *Damudoxylon*, *Kaokoxylon* and *Taeniopitys*. Rev. Palaeobot. Palynol. 195, 50–64.
Legendre, P., Legendre, L., 1998. Numerical Ecology. second ed. Elsevier, Amsterdam (853 pp.).
Lejal-Nicol, A., 1985. Carboniferous megafloras of North Africa. In: Martinez-Diaz, C. (Ed.), The Carboniferous of the World. I.G.M.E., Madrid, Tomo. vol. II, pp. 386–391.
Löcse, E., Meyer, J., Klein, R., Linnemann, U., Weber, J., Rößler, R., 2013. Neue Florenfunde in einem Vulkanit des Oberkarbons von Flöha. Veröffentlichungen des Museums für Naturkunde Chemnitz 36, 85–142.
Luthardt, L., Rößler, R., Schneider, J.W., 2015. Palaeoclimatic and site-specific conditions in the early Permian fossil forest of Chemnitz - Sedimentological, geochemical and palaeobotanical evidence. Palaeogeogr. Palaeoclimatol. Palaeoecol. 441, 627–652.
Martínek, K., Štolfova, K., 2009. Provenance study of Permian non-marine sandstones and conglomerates of the Krkonoše Piedmont Basin (Czech Republic): exotic marine limestone pebbles, heavy minerals and garnet composition. Bull. Geosci. 84, 1–14.
Matysová, P., Rößler, R., Götze, J., Leichmann, J., Forbes, G., Taylor, E.L., Sakala, J., Grygar, T., 2010. Alluvial and volcanic pathways to silicified plant stems (Upper Carboniferous–Triassic) and their taphonomic and environmental meaning. Palaeogeogr. Palaeoclimatol. Palaeoecol. 292, 127–143.
Merlotti, S., 2009. Reavaliação taxonômica de lenhos das formações Irati e Serra Alta, Permiano da Bacia do Paraná, Brasil. Pesquisas em Geociências 36, 11–21.
Merlotti, S., Kurzawe, F., 2011. Lenhos permianos da Bacia do Paraná, Brasil: síntese e revisão taxonômica. Gaea 7, 19–33.
Meyen, S.V., 1987. Fundamentals of Palaeobotany. Chapman & Hall Ltd, London (432 pp).
Montañez, I.P., Poulsen, C.J., 2013. The Late Paleozoic ice age: an evolving paradigm. Annu. Rev. Earth Planet. Sci. 41, 629–656.
Mussa, D., 1978a. *Brasilentiloxylon* e *Solenobrasilioxylon*, dois novos gêneros gondwânicos na Formação Irati, Estado de São Paulo. Boletim IG-USP 9, 118–127.
Mussa, D., 1978b. On the anatomy of wood showing affinities with the genus *Vertebraria* Royle, from the Irati formation, state of São Paulo, Brazil. Boletim IG-USP 9, 153–201.
Mussa, D., 1982. Lignitafofloras permianas da Bacia do Paraná (Estados de São Paulo e Santa Catarina). (Ph.D. Thesis). vol. 1. Instituto de Geociências - Universidade de São Paulo, São Paulo (463 pp).
Mussa, D., 1986. Eustelos gondwânicos de medulas diafragmadas e sua distribuição estratigráfica. Boletim IG-USP 17, 11–26.
Mussa, D., Coimbra, A.M., 1984. Método de estudo tafonômico aplicado a lignispécimes permianos da Bacia do Paraná. An. Acad. Bras. Cienc. 56, 85–101.
Mussa, D., Coimbra, A.M., 1987. Novas perspectivas de comparação entre as tafofloras permiannas (de lenhos) das bacias do Parnaíba e do Paraná. X Congresso Brasileiro de Paleontologia. Sociedade Brasileira de Paleontologia, Rio de Janeiro, pp. 901–923.
Mussa, D., Carvalho, R.G., Santos, P.R., 1980. Estudo estratigráfico e paleoecológico em ocorrências fossilíferas da Formação Irati, Estado de São Paulo, Brasil. Boletim IG-USP 11, 142–149.
Neregato, R., 2012. Esfenófitas do Monumento Natural das Árvores Fossilizadas do Tocantins, Bacia do Parnaíba (Permiano, Brasil). (Ph.D. Thesis). Instituto de Geociências e Ciências Exatas - Universidade Estadual Paulista "Júlio de Mesquita Filho", Rio Claro (189 pp).
Neregato, R., RößLer, R., Rohn, R., Noll, R., 2015. New petrified calamitaleans from the Permian of the Parnaíba Basin, central-north Brazil. Part I. Rev. Palaeobot. Palynol. 215, 23–45.
Noll, R., 2000. Ein zierlicher Calamit vom Donnersberg. Veröffentlichungen des Naturhistorischen Museums Schleusingen 24, 51–58.
Opluštil, S., Pšenika, J., Libertín, M., Bek, J., Daškova, J., Šimunek, Z., Drabkova, J., 2009. Composition and structure of an in situ Middle Pennsylvanian peat-forming plant assemblage buried in volcanic ash, Radnice Basin (Czech Republic). PALAIOS 24, 726–746.
Parrish, J.T., 1995. Geologic evidence of Permian climate. In: Scholle, P.A., Peryt, T.M., Ulmer-Scholle, D.S. (Eds.), The Permian of the Northern PangeaPaleogeography, Paleoclimates, Stratigraphy 1. Springer Verlag, Berlin, pp. 53–61.
Pelourde, F., 1914. A propos dês Psaroniées du Brésil. Association Française pour l'avancement des Sciences. Compte-rendu de la 43me session Le Havre (442–445 pp).
Petzholdt, A., 1841. Ueber Calamiten und Steinkohlenbildung. Arnoldische Buchhandlung, Dresden and Leipzig (68 pp).
Pfefferkorn, H.W., Archer, A.W., Zodrow, E.L., 2001. Modern tropical analogs for standing carboniferous forests: comparison of extinct *Mesocalamites* with extant *Montrichardia*. Hist. Biol. 15, 235–250.
Pinto, C.P., Sad, J.H.G., 1986. Revisão da estratigrafia da Formação Pedra de Fogo, borda sudoeste da Bacia do Parnaíba. XXXIV Congresso Brasileiro de Geologia. Sociedade Brasileira de Geologia, Goiânia, pp. 346–358.
Rees, P.M., Gibbs, M.T., Ziegler, A.M., Kutzbach, J.E., Behling, P.J., 1999. Permian climates: evaluating model predictions using global paleobotanical data. Geologija 27, 891–894.
Rees, P.M., Ziegler, A.M., Gibbs, M.T., Kutzbach, J.E., Behling, P.J., Rowley, D.B., 2002. Permian phytogeographic patterns and climate data/model comparisons. J. Geology 110, 1–31.
Renault, B., 1893. Bassin houiller et Permien d'Autun et d'Epinac. Études des gîtes minéraux de la France. Fascicule IV, Flore Fossile, 2. Partie. Paris, Atlas, 89 planches.
Renault, B., 1896. Bassin houiller et Permien d'Autun et d'Epinac. Études des gîtes minéraux de la France. Fascicule IV, Flore Fossile, 2. Partie. Paris, Texte (578 pp.).
Ricardi-Branco, F., 2008. Venezuelan paleoflora of the Pennsylvanian-Early Permian: paleobiogeographical relationships to central and western equatorial pangea. Gondwana Res. 14, 297–305.
Rohn, R., Rösler, O., 1987. Relações entre a flora permiana do Gondvana e as floras das províncias setentrionais. 2. X Congresso Brasileiro de Paleontologia. Sociedade Brasileira de Paleontologia, Rio de Janeiro, pp. 885–899.
Roscher, R.M., Schneider, J.W., 2006. Permo-Carboniferous climate: Early Pennsylvanian to Late Permian climate of central Europe in a regional and global context. In: Lucas, S.G., Cassins, G., Schneider, J.W. (Eds.), Non-marine Permian Biostratigraphy And Biochronology. The Geol. Soc. Spec. Publ. 265, London, pp. 95–136.
Rösler, O., 1978. The Brazilian Eogondwanic floral succession. Boletim IG-USP 9, 85–90.
Ross, C.A., Ross, J.R.P., 1985. Carboniferous and early Permian biogeography. Geologija 13, 27–30.
Rößler, R., 2006. Two remarkable Permian petrified forests: correlation, comparison and significance. In: Lucas, S.G., Cassinis, G., Schneider, J.W. (Eds.), Non-marine Permian Biostratigraphy and Biochronology. The Geological Society of London Spec. Publ. 265, London, pp. 39–63.
Rößler, R., 2014. Die Bewurzelung permischer Calamiten – Aussage eines Schlüsselfundes zur Existenz freistehender baumförmiger Schachtelhalmgewächse innerhalb der Paläofloren des äquatornahen Gondwana. Freiberger Forschungshefte C 548. Paläontologie, Stratigraphie, Fazies 22, 9–37.
Rößler, R., Galtier, J., 2002a. First *Grammatopteris* tree ferns from the Southern Hemisphere – new insights in the evolution of the Osmundaceae from the Permian of Brazil. Rev. Palaeobot. Palynol. 121, 205–230.
Rößler, R., Galtier, J., 2002b. Dernbachia brasiliensis gen. nov. et sp. nov. – a new small tree fern from the Permian of NE Brazil. Rev. Palaeobot. Palynol. 122, 239–263.
Rößler, R., Galtier, J., 2003. The first evidence of the fern *Botryopteris* from the Permian of the Southern Hemisphere reflecting growth form diversity. Rev. Palaeobot. Palynol. 127, 99–124.
Rößler, R., Noll, R., 2002. Der permische versteinerte Wald von Araguaina/Brasilien-Geologie, Taphonomie und Fossilführung. Veröffentlichungen des Naturhistorischen Museums Schleusingen 25, 5–44.
Rößler, R., Noll, R., 2006. Sphenopsids of the Permian (I): the largest known anatomically preserved calamite, an exceptional find from the petrified forest of Chemnitz, Germany. Rev. Palaeobot. Palynol. 140, 145–162.
Rößler, R., Noll, R., 2007. *Calamitea* Cotta, the correct name for calamitean sphenopsids currently classified as *Calamodendron* Brongniart. Rev. Palaeobot. Palynol. 144, 157–180.
Rößler, R., Noll, R., 2010. Anatomy and branching of *Arthopitys bistriata* (Cotta) – new observations from the Permian Petrified Forest of Chemnitz, Germany. Int. J. Coal Geol. 83, 103–124.
Rößler, R., Feng, Z., Noll, R., 2012. The largest calamite and its growth architecture – *Arthropitys bistriata* from the early Permian Petrified Forest of Chemnitz. Rev. Palaeobot. Palynol. 185, 64–78.
Rößler, R., Merbitz, M., Annacker, V., Noll, R., Neregato, R., Rohn, R., 2014. The root systems of Permian arborescent sphenopsids: evidence from both the northern and southern hemispheres. Palaeontogr. Abt. B 290, 65–107.
Santos, R.V., Souza, P.A., Alvarenga, C.J.S., Dantas, E.L., Pimentel, M.M., Oliveira, C.G., Araújo, L.M., 2006. Shrimp U-Pb zircon dating and palynology of bentonitic layers from the Permian Irati Formation, Paraná Basin, Brazil. Gondwana Res. 9, 456–463.
Scotese, C.S., 1999. Paleomap Project. Available at: http://www.scotese.com (Accessed in 10/11/2009).
Scotese, C.R., Barret, S.F., 1990. Gondwana's movement over the South Pole during the Palaeozoic: evidence from lithological indicators of climate. In: McKerrow, W.S., Scotese, C.R. (Eds.), Palaeozoic Palaeogeography and Biogeography. Geol. Soc. Memoir 12, London, pp. 94–123.
Scotese, C.R., Langford, R.P., 1995. Pangea and the paleogeography of the Permian. In: Scholle, P.A., Peryt, T.M., Ulmer-Scholle, D.S. (Eds.), The Permian of the Northern Pangea. Springer Verlag, Berlin, pp. 3–19.
Solms-Laubach, H., 1913. *Tietea singularis*, ein neuer fossiler Pteridineen-Stamm aus Brasilien. Zeitschr. Botanik 5, 673–700.
Tabor, N.J., Poulsen, C.J., 2008. Palaeoclimate across the Late Pennsylvanian-Early Permian tropical palaeolatitudes: a review of climate indicators, their distribution, and relation to palaeophysiographic climate factors. Palaeogeogr. Palaeoclimatol. Palaeoecol. 268, 293–310.

Tavares, T.M.V., 2011. Estudo de Marattiales da "Floresta Petrificada do Tocantins Setentrional" (Permiano, Bacia do Parnaíba). (Ph.D. Thesis). Instituto de Geociências e Ciências Exatas - Universidade Estadual Paulista "Júlio de Mesquita Filho", Rio Claro (184 pp).
Tavares, T.M.V., Rohn, R., Rößler, R., Feng, Z., Noll, R., 2014. Petrified Marattiales pinnae from the Lower Permian of North-Western Gondwana (Parnaíba Basin, Brazil). Rev. Palaeobot. Palynol. 201, 12–28.
Thomas, B.A., 2013. In situ stems: preservation states and growth habits of the Pennsylvanian (Carboniferous) calamitaleans based upon new studies of *Calamites* Sternberg, 1820 in the Duckmantian at Brymbo, North Wales, UK. Palaeontology 57, 21–36.
Wang, S.J., Li, S.S., Hilton, J., Galtier, J., 2003. A new species of sphenopsid stem *Arthropitys* from Late Permian volcaniclastic sediments of China. Rev. Palaeobot. Palynol. 126, 65–81.
Wang, S.J., Hilton, J., Galtier, J., Tian, B., 2006. A large anatomically preserved calamitean stem from the Upper Permian of southwest China and its implications for calamitean development and functional anatomy. Plant Syst. Evol. 261, 229–244.
Wnuk, C., 1996. The development of floristic provinciality during the Middle and Late Paleozoic. Rev. Palaeobot. Palynol. 90, 5–40.
Ziegler, A.M., Hulver, M.L., Rowley, D.B., 1997. Permian world topography and climate. In: Martini, I.P. (Ed.), Late Glacial and Postglacial Environments Changes: Quaternary, Carboniferous-Permian and Proterozoic. Oxford University Press, Oxford, pp. 111–146.

Further Reading

Caldas, E.B., Mussa, D., Lima-Filho, F.P., Rösler, O., 1989. Nota sobre a ocorrência de uma floresta petrificada de idade permiana em Teresina, Piauí. Boletim IG-USP, Publicação Especial 7, 69–87.